HMGB1–RAGE regulates muscle satellite cell homeostasis through p38-MAPK- and myogenin-dependent repression of *Pax7* transcription

Francesca Riuzzi*, Guglielmo Sorci*, Roberta Sagheddu and Rosario Donato‡

Department of Experimental Medicine and Biochemical Sciences and Istituto Interuniversitario di Miologia, University of Perugia, Via del Giochetto, 06122, Perugia, Italy

*These authors contributed equally to this work
‡Author for correspondence (donato@unipg.it)

Accepted 29 October 2011
Journal of Cell Science 125, 1440–1454

doi: 10.1242/jcs.092163

Summary

Expression of the paired-box 7 (PAX7) transcription factor is regulated during both myoblast proliferation and differentiation: high levels of PAX7 compromise myogenic differentiation because of excess and prolonged proliferation, whereas low levels of PAX7 result in precocious differentiation. We showed that myogenin repressed *Pax7* transcription in differentiating myoblasts by binding to specific recognition sites in the *Pax7* promoter, and that high-mobility group box 1 (HMGB1)–receptor for advanced glycation end-products (RAGE) signaling was required for myogenin induction and myogenin-dependent repression of *Pax7* transcription. In addition, PAX7 negatively and myogenin positively regulated RAGE expression. RAGE, a multiligand receptor of the immunoglobulin superfamily, was not expressed in adult skeletal muscles, and was transiently expressed in activated, proliferating and differentiating satellite cells (SCs) in injured muscles. Compared with wild-type muscles, $Rage^{-/-}$ muscles exhibited increased numbers of basal SCs that were further increased in injured $Rage^{-/-}$ muscles following elevated myoblast asymmetric division; complete regeneration of injured $Rage^{-/-}$ muscles was found to be delayed by ~1 week. Thus, RAGE signaling physiologically repressed *Pax7* transcription in SCs by upregulating myogenin, thereby accelerating muscle regeneration and limiting SC self-renewal.

Key words: Muscle regeneration, Satellite cell, PAX7, Myogenin, HMGB1–RAGE

Introduction

Myogenesis is a multistep process orchestrated and regulated by several intracellular and extracellular factors (Brack et al., 2007; Buckingham, 2006; Chargé and Rudnicki, 2004; Kuang et al., 2008). Among the intracellular factors involved in this process are transcription factors, some of which (i.e. MYF5, MYOD, myogenin and MRF4) are muscle specific. These are activated and inactivated in a timely manner to ensure a highly ordered succession of events leading to myofiber formation. By contrast, the extracellular factors involved are signals that act in an autocrine, paracrine and endocrine manner via activation of cell surface receptors. A hierarchy of transcription factors has been delineated in which the transcription factors paired-box 3 (PAX3) and/or PAX7 regulate MYF5, which in turn regulates MYOD. MYF5 and MYOD can independently regulate myogenin, which is indispensable for myoblast terminal differentiation (Buckingham, 2006; Chargé and Rudnicki, 2004). Central to adult myogenesis are quiescent, mononucleated cells located between the sarcolemma and the basal lamina of myofibers [so-called 'satellite cells' (SCs)]: following intense physical exercise, trauma, inflammatory processes or muscle wasting consequent to chronic inflammatory processes, sepsis or cancer, and in muscular dystrophies, SCs exit quiescence, proliferate and eventually fuse with each other to either form new myofibers and/or repair damaged ones (Brack et al., 2007; Buckingham, 2006; Chargé and Rudnicki, 2004; Kuang et al., 2008; Tedesco et al., 2010). To reconstitute the SC reserve pool, some myoblasts have to stop proliferation without undergoing differentiation or apoptosis; in so doing, these cells reacquire a quiescent state.

PAX7 is expressed in, and marks, quiescent and proliferating SCs and myoblasts and is repressed in differentiating myoblasts (Collins et al., 2009; Relaix et al., 2005; Relaix et al., 2006; Seale et al., 2000). The expression of PAX7 and myogenin is mutually exclusive in SCs and myoblasts: downregulation of PAX7 is required for myoblast terminal differentiation, and sustained expression of PAX7 in SCs delays the onset of myogenesis and stimulates acquisition of a quiescent state (Olguin and Olwin, 2004; Zammit et al., 2004). By contrast, PAX7 is essential not only for the formation of functional myogenic progenitors, stimulating their proliferation and survival, and preventing their precocious differentiation, but also for SC self-renewal (Kuang et al., 2006). Therefore, regulation of PAX7 is crucial for the transition of SCs from proliferation to self-renewal or differentiation. There is evidence that MYOD and myogenin downregulate PAX7 post-translationally (Olguin et al., 2007) and that microRNA-1, microRNA-206 and microRNA-486 downregulate PAX7 post-transcriptionally (Chen et al., 2010; Dey et al., 2011) in myoblasts committed to differentiation. However, it is not known whether myogenin affects *Pax7* transcription.

The receptor for advanced glycation end-products (RAGE), a member of the immunoglobulin superfamily (Bierhaus et al., 2005; Schmidt et al., 2001), is expressed in cultured myoblast cell lines and primary myoblasts but not in mature myofibers (Sorci et al., 2003; Sorci et al., 2004). When activated in myoblasts by its

ligand, high mobility group box 1 (HMGB1) (Bianchi and Manfredi, 2007; Rauvala and Rouhiainen, 2007), RAGE transduces a pro-myogenic, antiproliferative and antitumor signal through activation of a Cdc42–Rac1–MKK6–p38-MAPK–myogenin axis and inactivation of the mitogenic ERK1/2 and JNK (Riuzzi et al., 2006; Riuzzi et al., 2007; Sorci et al., 2004). However, whether RAGE signaling physiologically participates in myogenesis remains to be determined.

We show here that myogenin repressed *Pax7* transcription by binding to regulatory sequences in the *Pax7* promoter, and that an HMGB1–RAGE axis was required for myogenin to repress *Pax7* transcription. We also show that *Rage*$^{-/-}$ myoblasts exhibited high levels of PAX7, enhanced proliferation and reduced differentiation compared with wild-type (WT) myoblasts, and that deletion of *Rage* promoted myoblast asymmetric division. Lastly, we demonstrate that RAGE became transiently expressed in SCs in injured muscles, and that *Rage*$^{-/-}$ muscles showed larger SC numbers; in addition, completion of their regeneration following injury was delayed compared with WT muscles. Thus, *Pax7* is transcriptionally modulated by myogenin, and RAGE signaling physiologically downregulates PAX7 expression by upregulating myogenin in activated SCs, thereby reducing SC proliferation, avoiding excess SC self-renewal and accelerating myogenic differentiation.

Results

Inverse relationship between the expression of RAGE and myogenin and that of PAX7 in myoblasts

Switching C2C12 myoblasts, an established SC model, from growth medium (GM) to differentiation medium (DM) resulted in a time-dependent increase in PAX7 mRNA and protein levels with maximum levels at 16 hours, followed by a robust reduction at 24 and 48 hours (Fig. 1A). Compared with the GM condition, myogenin levels increased in DM after 1 hour (mRNA) and after 3 hours (protein), with high myogenin protein levels during the 8–48-hour interval (Fig. 1A); RAGE mRNA and protein levels increased in DM compared with GM in a similar pattern to that of myogenin (Fig. 1A). Thus, high RAGE and myogenin levels coincided with low PAX7 levels at 24 and 48 hours in DM; however, from 2 hours to 16 hours in DM, PAX7, myogenin and RAGE were expressed at relatively high levels.

In GM, 100% of myoblasts were RAGE^{+} (Fig. 1B; supplementary material Fig. S1A,C) and ~90% were PAX7^{+} (Fig. 1B; supplementary material Fig. S1A,B); at 3 hours and 6 hours by the switch to DM RAGE was found in 100% of myoblasts, myogenin in ~15% and ~25% of cells, respectively, and PAX7 in ~70% and ~65% of cells, respectively, with nearly all myogenin^{+} cells being PAX7^{+} cells at both 3 hours and 6 hours (Fig. 1B; supplementary material Fig. S1B,C). At 24 hours in DM, RAGE, myogenin and PAX7 were found in 100%, ~50% and ~20% of myoblasts, respectively (Fig. 1B; supplementary material Fig. S1A–C). At 48 hours, PAX7 was found in ~15% of mononucleated cells and myogenin was found in myotubes and ~85% of mononucleated cells. At 6 days in DM, RAGE and myogenin were coexpressed at high levels in myotubes, RAGE was found in myogenin^{+} myoblasts, and PAX7 was restricted to those myoblasts that were myogenin^{-} and only slightly RAGE^{+} (Fig. 1B; supplementary material Fig. S1A–C). These latter cells were probably myoblasts on the way to become quiescent (Yoshida et al., 1998), whereas RAGE^{+}–myogenin^{+} cells were myocytes committed to fusion, a conclusion supported by the finding that, at 6 days, a small percentage (~1%) of myoblasts were BrdU^{+}, that is, proliferating (supplementary material Fig. S1D). Notably, starting at 16 hours with the switch to DM, myogenin and PAX7 were no longer coexpressed in most cells and, at very early (i.e. 3 hours) and late (i.e. 6 days) stages, myogenin^{+} cells exhibited a stronger RAGE fluorescence signal than did myogenin^{-} cells (supplementary material Fig. S1A–C). These results pointed to an inverse relationship between the expression of RAGE and myogenin and that of PAX7 in myocytes, and suggested that a RAGE–myogenin axis downregulates PAX7 at early differentiation stages and that PAX7 expression negatively regulates RAGE expression in myogenin^{-} myoblasts at late differentiation stages.

Downregulation of PAX7 is dependent on levels of RAGE and myogenin, and on HMGB1

Treatment of C2C12 myoblasts in DM with a RAGE-neutralizing antibody resulted in increased PAX7 levels and reduced myogenin levels. These effects were observed as early as 6 hours with the transfer of myoblasts from GM to DM (Fig. 1C,D). Treatment of myoblasts in DM with the RAGE activator, HMGB1, resulted in increased myogenin levels and reduced PAX7 levels (Fig. 1C–E), whereas treatment with BoxA, a specific HMGB1 antagonist (Anderson et al., 2002), resulted in reduced myogenin levels and enhanced PAX7 levels (Fig. 1E). Also, ectopic RAGE expression in C2C12 myoblasts resulted in reduced PAX7 levels and enhanced myogenin levels in both GM and DM, whereas ectopic expression of the dominant negative RAGE mutant, RAGEΔcyto, resulted in the opposite (Fig. 1F). In agreement with the notion that p38 MAPK (MAPK14) regulates the expression of PAX7 and myogenin (de Angelis et al., 2005; Palacios et al., 2010; Perdiguero et al., 2007; Serra et al., 2007), treatment of myoblasts in DM with the p38 MAPK inhibitor, SB203580, resulted in reduced myogenin levels and robust upregulation of PAX7 levels (supplementary material Fig. S2A,B).

We then examined whether changes in myogenin abundance impacted PAX7 levels. Ectopic myogenin expression in C2C12 myoblasts resulted in a robust decrease in PAX7 mRNA and protein levels and in a dose-dependent reduction of *Pax7* transcription as examined by double transfection with a myogenin expression vector and a luciferase reporter vector under the control of the –4800 bp region of the human *PAX7* promoter (Murmann et al., 2000), even in GM (Fig. 1G). Conversely, transfection with myogenin siRNA resulted in significant suppression of myotube formation and increased PAX7 mRNA and protein levels in DM (Fig. 1H). Thus, *Pax7* transcription and PAX7 protein levels were regulated by levels of RAGE and myogenin and by HMGB1.

Myogenin binds to regulatory sequences in the *Pax7* promoter in a RAGE-dependent manner

We asked whether, in addition to post-transcriptional (Chen et al., 2010; Dey et al., 2011) and post-translational (Olguin et al., 2007) regulation, PAX7 is regulated by a transcriptional mechanism and whether RAGE signaling has a role in this regulation. The promoter of mouse *Pax7* contains six putative myogenin recognition sites (5′-TGCCTGG-3′, Path^{TM} public 1.0 pattern search for transcription factor binding sites). As investigated by chromatin-immunoprecipitation (ChIP) in C2C12 myoblasts, myogenin bound to sites 1, 3, 5 and 6 in

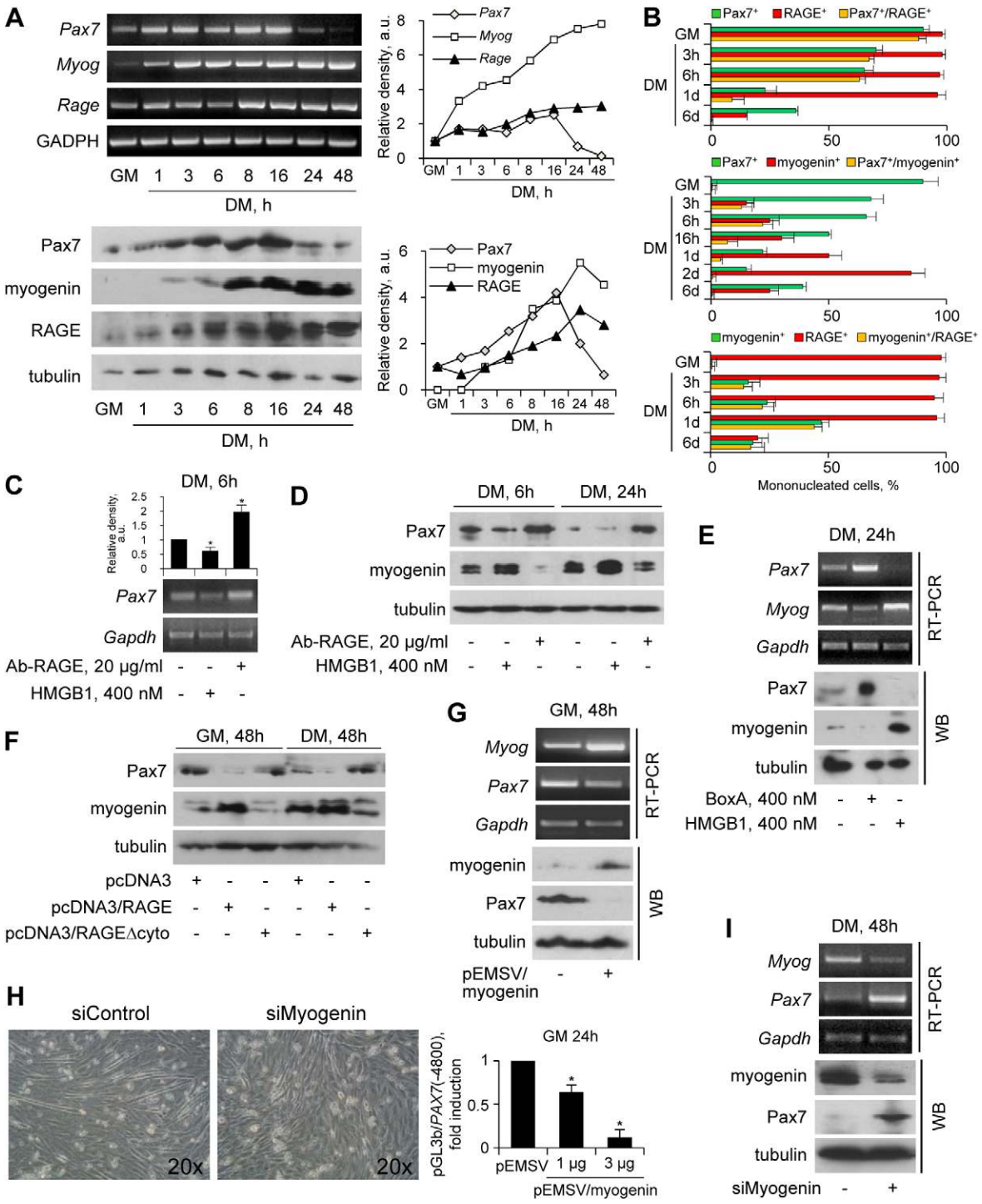

Fig. 1. HMGB1–RAGE signaling-dependent myogenin expression downregulates PAX7 expression in differentiating myoblasts. (**A**) C2C12 myoblasts were cultivated for 24 hours in GM and then transferred to DM. At intervals, cells were analyzed by RT-PCR (top panel) or western blotting (bottom panel) to detect PAX7, myogenin and RAGE. (**B**) C2C12 myoblasts were grown on glass coverslips, fixed and subjected to double immunofluorescence using the antibodies indicated. For each condition, the percentage of positive cells is given as the mean ± standard deviation (SD) of total counts in 20 randomly chosen fields. (**C**) Same as in A except that myoblasts were treated with either a RAGE-neutralizing antibody or HMGB1. After 6 hours in DM, cells were analyzed for expression of *Pax7* by RT-PCR. (**D**) Same as in C except that, after 6 and 24 hours in DM, cell lysates were analyzed for PAX7 and myogenin levels by western blotting. (**E**) Same as in C and D except that cells were treated with either HMGB1 or the HMGB1 inhibitor, BoxA, and analyzed for levels of PAX7 and myogenin by RT-PCR and western blotting. (**F**) C2C12 myoblasts were transfected with a RAGE, a RAGEΔcyto expression vector or an empty vector in GM and cultivated in either GM or DM. Cell lysates were analyzed for PAX7 and myogenin levels by western blotting. (**G**) C2C12 myoblasts in GM were transiently transfected with a myogenin expression vector and analyzed for myogenin and PAX7 expression levels by RT-PCR (top panel) and western blotting (middle panel). C2C12 myoblasts in GM were double transfected with a myogenin expression vector and pGL3B–*PAX7*(-4800)-luc (see main text), cultivated for 48 hours in GM and subjected to luciferase assay (bottom panel). (**H**,**I**) C2C12 myoblasts in DM were transiently transfected with myogenin siRNA for 48 hours and then cultivated in DM for another 48 hours. Cultures were analyzed by phase-contrast microscopy (H) and for myogenin and PAX7 expression levels by RT-PCR and western blotting (I). *Significantly different from control (n=3).

GM and to all six sites in DM (Fig. 2A). Treatment of C2C12 myoblasts in DM with a RAGE-neutralizing antibody resulted in myogenin binding to site 1 only (Fig. 2A). By contrast, in primary WT myoblasts, myogenin bound to the six recognition sites of the *Pax7* promoter in DM and to site 1 and less abundantly to sites 5 and 6 in GM, whereas in *Rage*$^{-/-}$ myoblasts, myogenin did not bind to any of the six sites in GM and only bound to site 1 in DM (Fig. 2B). Differences between the amounts of bound myogenin in WT myoblasts compared with C2C12 myoblasts in GM might be the result of different amounts of expressed myogenin. Thus, myogenin repressed *Pax7* transcription in DM by associating with regulatory sequences in the *Pax7* promoter, and RAGE signaling was required for myogenin to repress *Pax7* transcription.

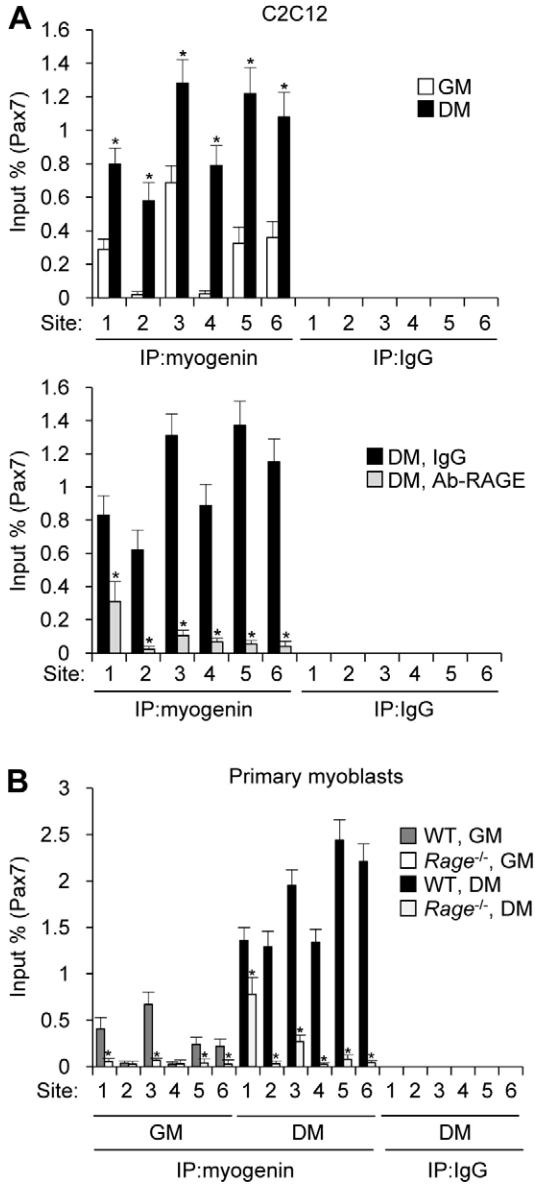

Fig. 2. Myogenin associates with regulatory sequences in the *Pax7* promoter in a RAGE-dependent manner. (**A**) C2C12 myoblasts were cultivated for 48 hours in either GM or DM (top panel). Parallel C2C12 myoblasts (bottom panel) were cultivated for 48 hours in DM in the presence of a RAGE-neutralizing antibody or non-immune IgG. Cells were then subjected to a ChIP assay using an anti-myogenin antibody. (**B**) WT and *Rage*$^{-/-}$ primary myoblasts cultivated in GM or DM were subjected to a ChIP assay using an anti-myogenin antibody. DNA obtained by ChIP was analyzed by real-time PCR. *Significantly different from control (n=3).

RAGE signaling promotes myoblast symmetric division

We next investigated whether RAGE and/or myogenin-dependent reduction of PAX7 levels impacts myoblast proliferation and differentiation. Isolation of myoblasts from neonatal limb muscles yielded approximately twice as many cells from *Rage*$^{-/-}$ mice as from WT mice (supplementary material Fig. S3A). Compared with WT myoblasts, *Rage*$^{-/-}$ myoblasts showed a higher proliferation rate in GM and DM (Fig. 3A), higher PAX7 and phosphorylated ERK1/2 levels, reduced levels of myogenin, myosin heavy chain (MyHC) and phosphorylated p38 MAPK (Fig. 3B), and defective differentiation (Fig. 3C). However, ectopic RAGE expression in *Rage*$^{-/-}$ myoblasts resulted in stimulation of myotube formation and high myogenin and phosphorylated p38 MAPK levels, and dramatically reduced PAX7 levels compared with mock-transfected myoblasts (Fig. 3D). Thus, RAGE expression was required for p38 MAPK–myogenin-dependent reduction of PAX7 levels and proliferation rate, and for activation of the myogenic program.

Downregulation of PAX7 is required for myogenic differentiation (Olguin and Olwin, 2004), and a role of PAX7 in the asymmetric division in SC maintenance has been documented (Kuang et al., 2008). Thus, we asked whether RAGE signaling regulates the way that myoblasts divide, either symmetrically or asymmetrically. Using fluorescence-activated cell sorting (FACS) and epifluorescence, we analyzed WT and *Rage*$^{-/-}$ myoblasts during successive divisions after loading with the fluorescent probe, Vybrant DiI (Krishnamurthy et al., 2008) (Fig. 3E). In the case of WT myoblasts, we observed a single population of fluorescent cells exhibiting decreasing fluorescence intensity over time. By contrast, in the case of *Rage*$^{-/-}$ myoblasts, a second population of non-fluorescent cells was generated over time, such that at day 6, ~10% of cells were fluorescent (albeit with reduced fluorescence intensity) and ~90% were non-fluorescent. An analysis of the percentage population of cell pairs (i.e. telophase cells) at day 2 in GM indicated that Vybrant DiI was distributed symmetrically and asymmetrically in ~87% and ~13% of WT myoblast pairs, respectively, and in ~57% and ~43% of *Rage*$^{-/-}$ myoblast pairs, respectively (Fig. 3E). Thus, RAGE signaling promoted myoblast symmetric division probably via myogenin-dependent reduction of PAX7 levels, which might impact SC self-renewal.

PAX7 negatively and myogenin positively regulate RAGE expression

Primary myoblasts in quiescence medium (QM) (Kitzmann et al., 1998) showed little, if any RAGE expression (Fig. 4A), and switching the cells to GM, which causes activation of quiescent myoblasts (Kitzmann et al., 1998), resulted in enhanced PAX7 protein levels and upregulation of RAGE (Fig. 4A). Switching myoblasts from QM to DM also resulted in a time-dependent increase in RAGE levels and decrease in PAX7 levels (Fig. 4A). Thus, the expression of PAX7 and of RAGE was mutually exclusive in myoblasts, except in GM and during early phases of myogenic differentiation, where the two proteins were

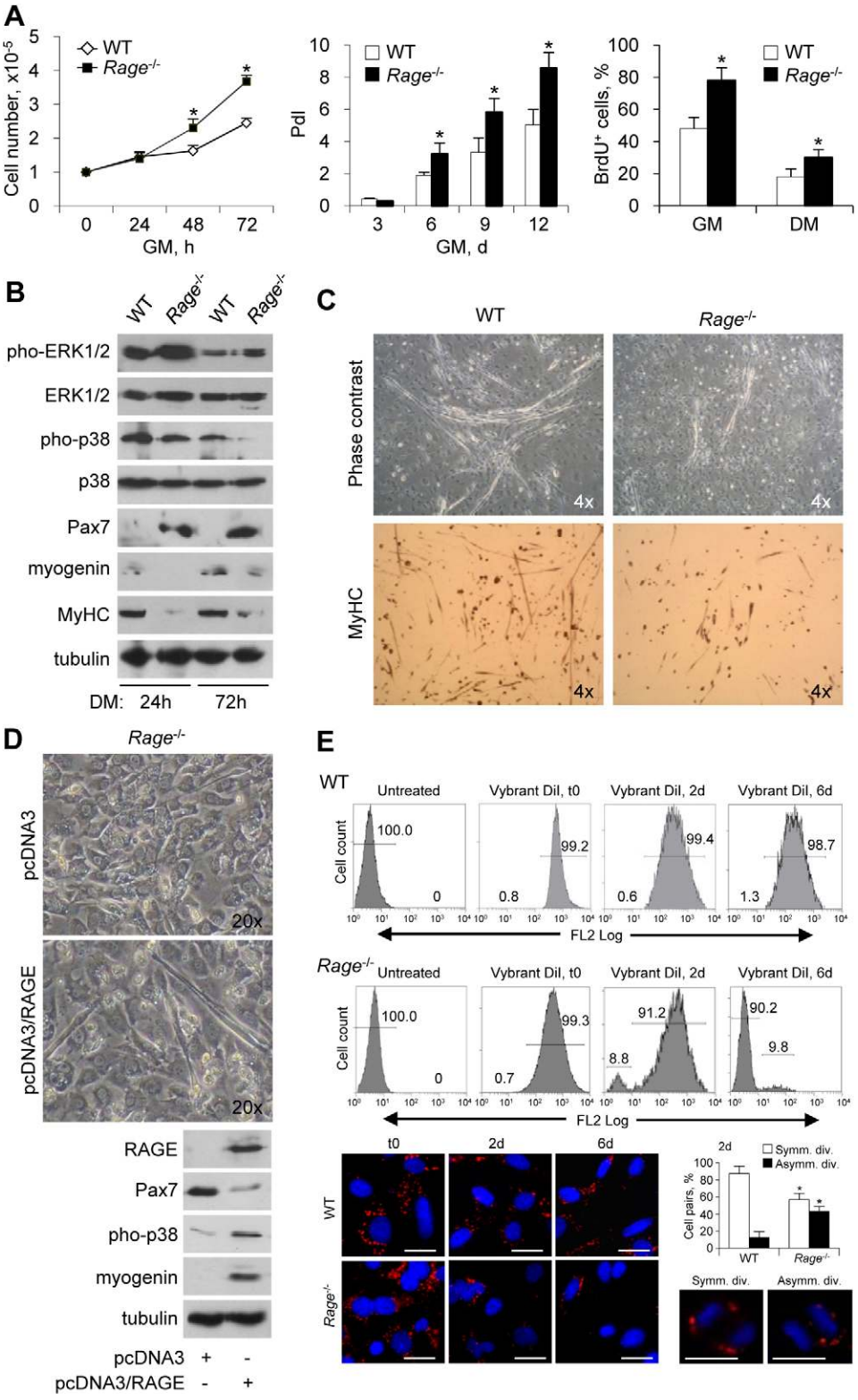

Fig. 3. *Rage*$^{-/-}$ myoblasts show an enhanced proliferation rate, elevated asymmetric division and defective differentiation compared with WT controls. (**A**) WT and *Rage*$^{-/-}$ myoblasts in GM were either counted at the indicated time points (left), analyzed for pdl (middle), or subjected to a BrdU incorporation assay (right). (**B**) WT and *Rage*$^{-/-}$ myoblasts were cultivated in DM and analyzed for PAX7, myogenin and MyHC levels and for p38 MAPK and ERK1/2 phosphorylation levels by western blotting. (**C**) WT and *Rage*$^{-/-}$ myoblasts were cultivated for 4 days in DM and analyzed by phase-contrast microscopy and MyHC immunocytochemistry. (**D**) *Rage*$^{-/-}$ myoblasts were transfected with a RAGE expression vector or an empty vector and cultivated for 2 days in DM. Cells were analyzed by phase-contrast microscopy or by western blotting for levels of PAX7, myogenin and RAGE. (**E**) WT and *Rage*$^{-/-}$ myoblasts were loaded with either vehicle or Vybrant DiI, and cultivated in GM. At intervals, cells were collected and subjected to FACS analysis (top panel). Shown are representative images of Vybrant DiI-loaded myoblasts (bottom left panel) and of cell pairs showing symmetric or asymmetric distribution of Vybrant DiI at day 2 in GM along with their quantification (bottom right panel). *Significantly different from control (n=3). Scale bars: 50 μm (E, bottom left panel); 20 μm (E, bottom right panel).

coexpressed (Fig. 1B; supplementary material Fig. S1A), and levels of functional RAGE in myoblasts correlated positively with myogenin levels and negatively with PAX7 levels.

The *Rage* promoter contains putative Pax (5′-GTGAC-3′) and myogenin (5′-TGCCTGG-3′) recognition sites (Path^{TM} public 1.0 pattern search for transcription factor binding sites). We found that cultivation of C2C12 myoblasts in DM for 2 days in the presence of the p38 MAPK inhibitor, SB203580, resulted in inhibition of myotube formation (supplementary material Fig. S2C,D), elevated PAX7 levels (Fig. 4B; supplementary material Fig. S2A,B,D) and reduced myogenin levels (Fig. 4B; supplementary material Fig. S2A–C) as expected, and a robust

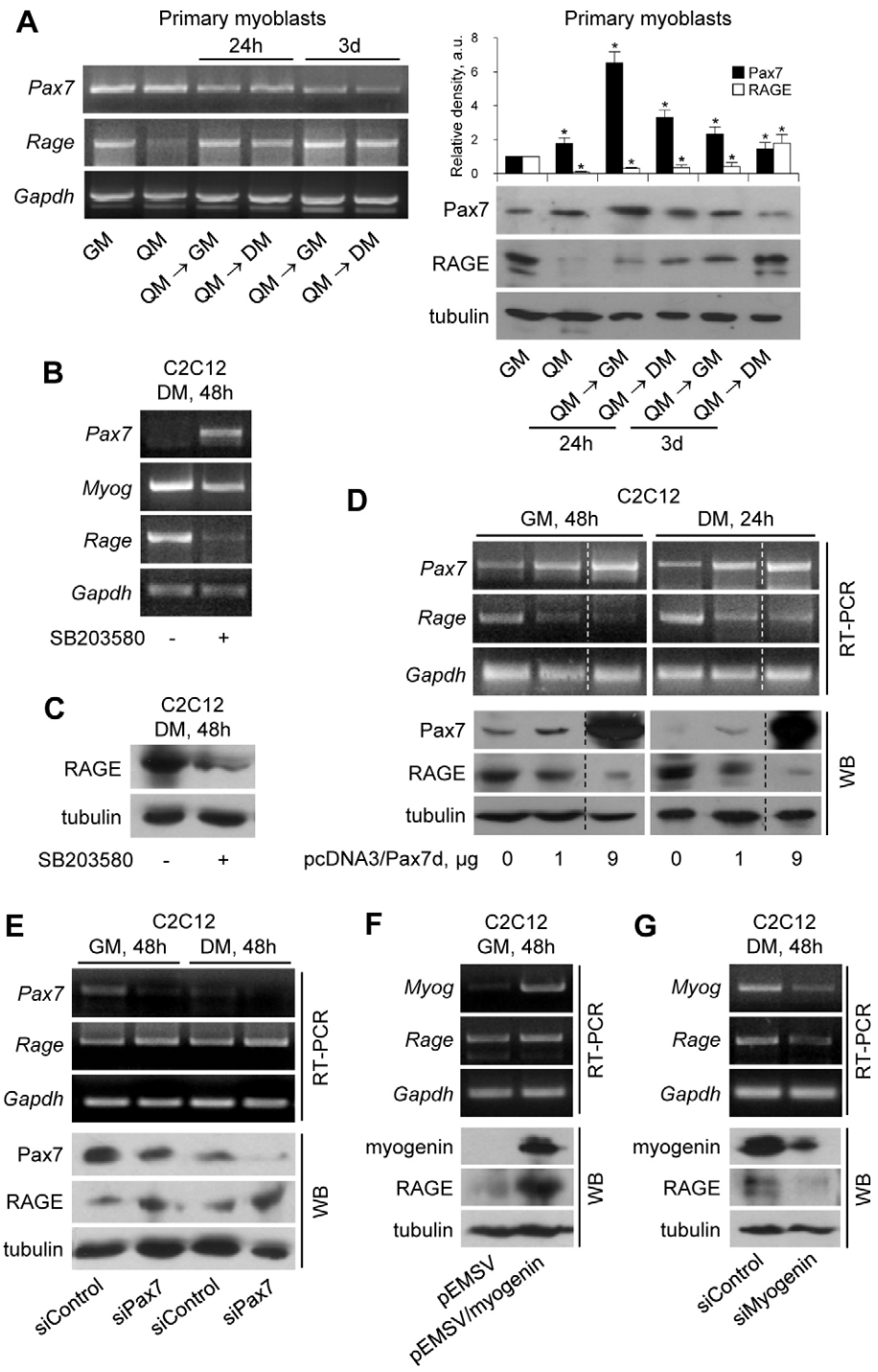

Fig. 4. PAX7 and myogenin regulate RAGE expression negatively and positively, respectively. (**A**) Primary myoblasts were cultivated in QM (2 days) and transferred to GM (1 day) or to DM for 3 days. Cells were analyzed for expression of PAX7, RAGE and myogenin by RT-PCR and western blotting. (**B**,**C**) C2C12 myoblasts were cultivated in DM in the absence or presence of SB203580. Cells were analyzed for expression of *Rage*, *Myog* and *Pax7* by RT-PCR (B) and for RAGE levels by western blotting (C). (**D**) C2C12 myoblasts were transiently transfected with PAX7 expression vector and cultivated in GM or DM. Cells were analyzed for expression of *Pax7* and *Rage* levels by RT-PCR and by western blotting. (**E**) C2C12 myoblasts were transiently transfected with PAX7 siRNA in DM (16 hours) and cultivated in DM. Cells were analyzed for expression of RAGE and PAX7 by RT-PCR and western blotting. (**F**) C2C12 myoblasts were transiently transfected with myogenin expression vector or empty vector for 2 days in GM, and analyzed for the expression of RAGE and myogenin by RT-PCR and western blotting. (**G**) C2C12 myoblasts were transiently transfected with myogenin siRNA or control siRNA in DM and cultivated in DM. Cells were analyzed for the expression of RAGE and myogenin by RT-PCR and western blotting.

decrease in RAGE levels (Fig. 4B,C; supplementary material Fig. S2C,D), compared with controls. Thus, relatively high PAX7 levels in DM, as obtained by inhibition of p38 MAPK, correlated positively with reduced RAGE levels in myoblasts. These results suggested that: (1) RAGE expression in myoblasts in DM was dependent on p38 MAPK; (2) the stimulation of p38 MAPK that occurs upon switching myoblasts from GM to DM was required for enhancement of RAGE expression; and (3) RAGE signaling via p38 MAPK might also serve to enhance RAGE expression in differentiating myoblasts. Moreover, ectopic PAX7 transfection resulted in reduced RAGE levels in GM and DM (Fig. 4D). Conversely, knockdown of PAX7 expression by RNA interference resulted in higher RAGE levels in GM and DM compared with controls (Fig. 4E). By contrast, compared with controls, RAGE levels in GM were higher in myogenin-transfected myoblasts and lower in DM in myogenin siRNA-treated myoblasts (Fig. 4F,G). Thus, myogenin induced by RAGE signaling to p38 MAPK upregulated RAGE expression by a positive feedback mechanism, whereas PAX7 downregulated RAGE expression.

RAGE is transiently expressed in regenerating skeletal muscles

We then determined whether RAGE signaling impacts skeletal muscle regeneration. RAGE was not expressed in adult mouse muscle tissue (Fig. 5A,B); however, RAGE became expressed in injured muscle tissue and was repressed at completion of regeneration (Fig. 5B,C). RAGE became detectable by western blotting by day 1 post-injury, was maximally expressed between days 3 and 7 post-injury, and was no longer expressed by day 28 post-injury (Fig. 5B). RAGE was found in mononucleated PAX7^{+} and mononucleated myogenin^{+} cells early after injury (Fig. 5C) and within regenerating myofibers recognized by their centrally located nuclei (Fig. 5B), probably as a result of expansion of RAGE^{+}–PAX7^{+} myoblasts (Fig. 5C) and fusion of RAGE^{+}–myogenin^{+} myoblasts (Fig. 5C). A fraction of RAGE^{+}–PAX7^{-}–myogenin^{-} cells in the degenerating tissue (Fig. 5Ca,c) were infiltrating macrophages (supplementary material Fig. S3E). It is known that RAGE is abundantly expressed in activated macrophages (Bierhaus et al., 2005; Schmidt et al., 2001).

Delayed muscle regeneration of injured *Rage*$^{-/-}$ muscles

Next, we examined the effects of *Rage* deletion on muscle regeneration. *Rage*$^{-/-}$ mice show no phenotype or motor disturbances. However, compared with WT controls, uninjured adult *Rage*$^{-/-}$ muscles exhibited ~40% more PAX7^{+} SCs (Fig. 6A), were reduced in number by ~26% and exhibited a

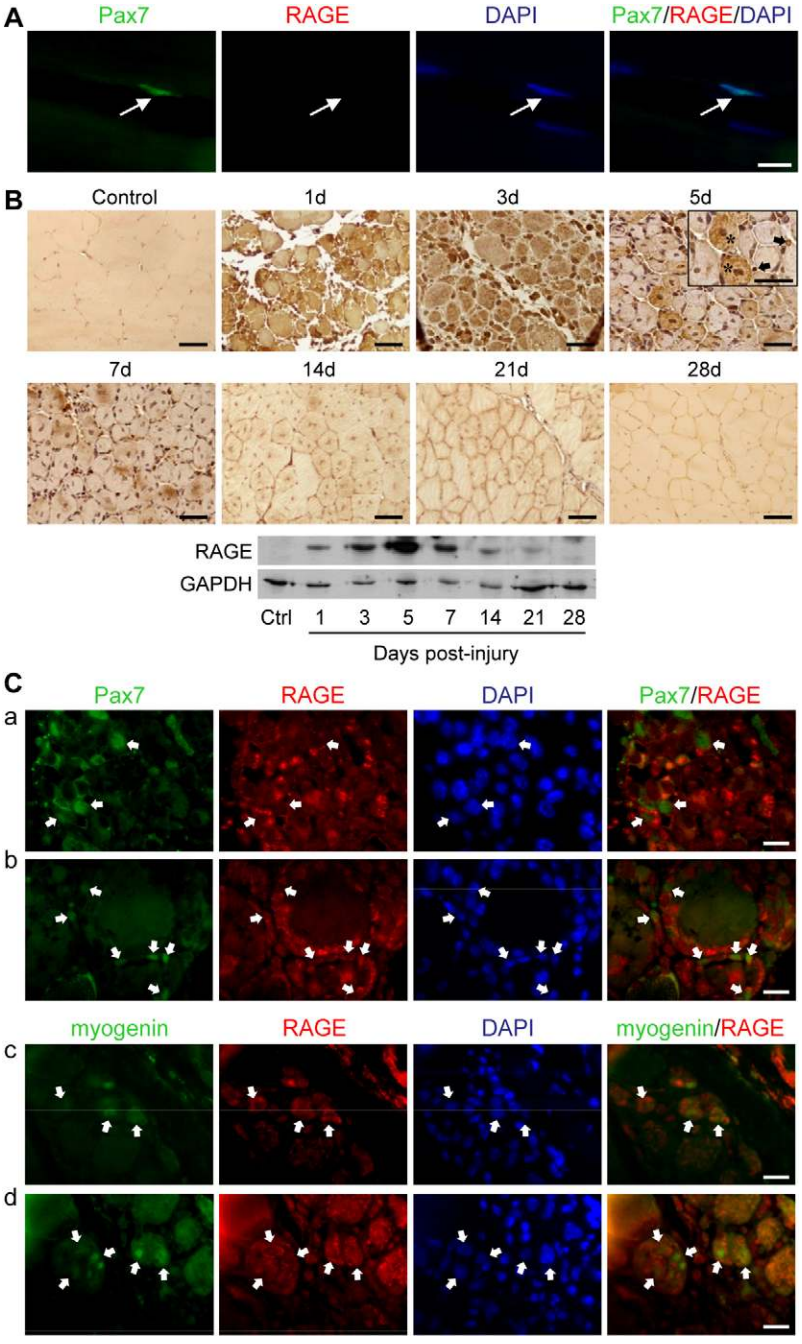

Fig. 5. Transient expression of RAGE in degenerating and/or regenerating myofibers. (**A**) Adult mouse muscle tissue was analyzed by double immunofluorescence using anti-PAX7 and anti-RAGE antibodies. (**B**) Immunohistochemical detection of RAGE in uninjured and degenerating and/or regenerating muscle tissue. RAGE is not found in uninjured tissue. At days 1–5 post-injury, RAGE is seen in isolated cells outside myofibers (arrows in inset) and within regenerating myofibers (asterisks in inset). By day 28 post-injury, regeneration is almost complete and no RAGE immune reaction product can be seen, as also shown by western blot analysis of whole-muscle homogenates. (**C**) Double immunofluorescence of PAX7 and RAGE (a,b) and myogenin and RAGE (c,d) at day 3 post-injury. Arrows indicate sparse PAX7^{+}–RAGE^{+} cells (a), PAX7^{+}–RAGE^{+} cells located at the periphery of regenerating myofibers (b) probably representing proliferating myoblasts, sparse myogenin^{+}–RAGE^{+} cells (c), and myogenin^{+}–RAGE^{+} cells located within regenerating myofibers (d). Nuclei were counterstained with DAPI. Scale bars: 20 μm (A), 200 μm (B) and 100 μm (C).

larger mean cross-sectional area (Fig. 6B,E); in addition, muscle tissue homogenates from *Rage*$^{-/-}$ adult mice contained larger amounts of PAX7 and MYF5, with an absence of MYOD expression in either case (supplementary material Fig. S3A).

Whereas in WT muscles regeneration was almost complete between days 14 and 21 post-injury (Fig. 5B; Fig. 6B), completion of regeneration of *Rage*$^{-/-}$ muscles lagged by at least 1 week, as shown by the longer degeneration phase (Fig. 6B, post-injury days 5 and 7), and the higher percentage of centrally nucleated myofibers at days 21 and 28 post-injury compared with WT muscles (Fig. 6B,C). In addition, the number of PAX7^{+} cells was significantly higher in *Rage*$^{-/-}$ muscles than in WT muscles at any time point during degeneration and/or regeneration (Fig. 6D). Compared with WT myofibers (Fig. 6E), at day 7 post-injury, *Rage*$^{-/-}$ myofibers were intermingled with a larger number of mononucleated cells, were reduced in number

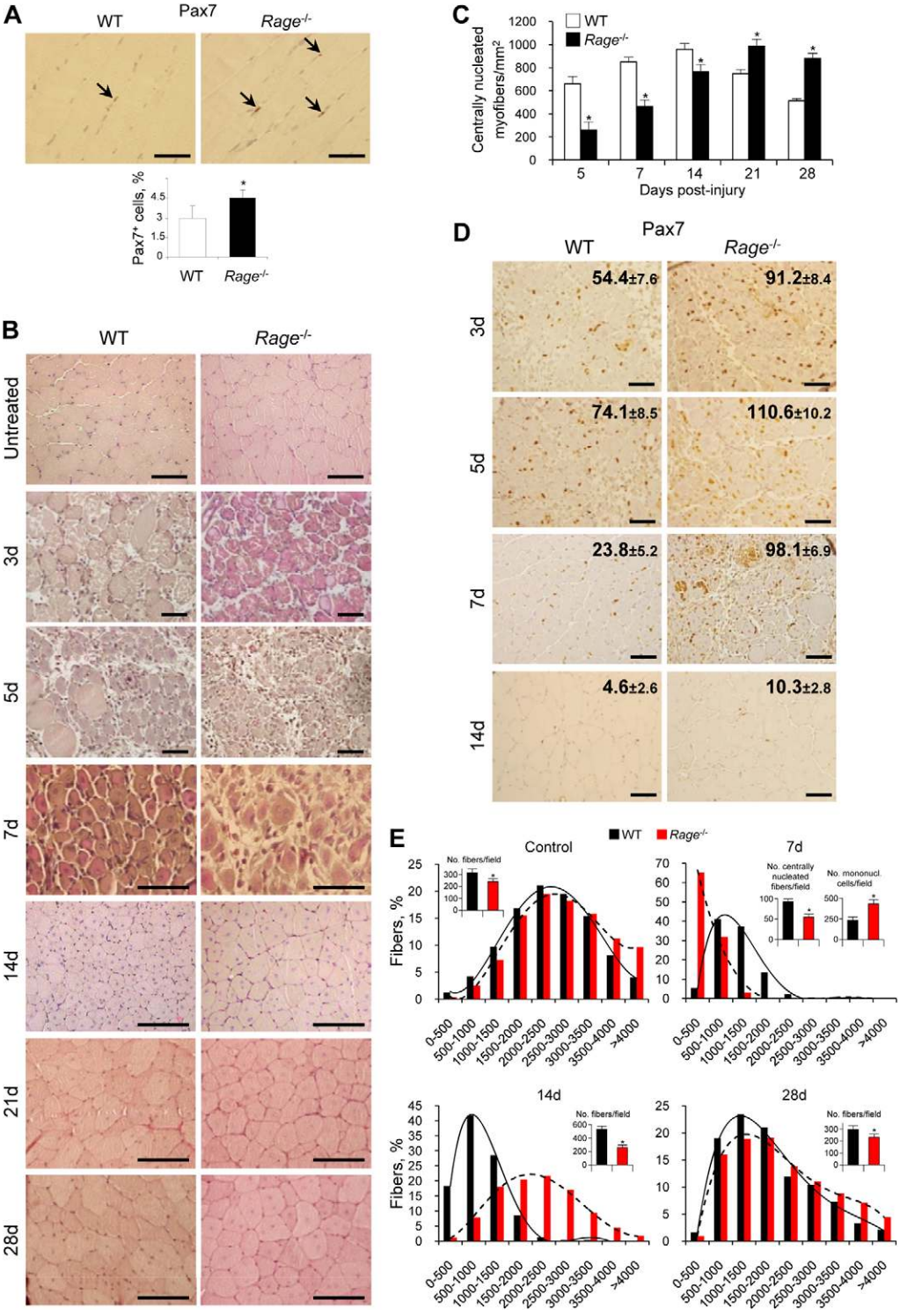

Fig. 6. Delayed muscle regeneration in *Rage*$^{-/-}$ muscles. (**A**) PAX7^{+} (satellite) cells (arrows) in uninjured WT and *Rage*$^{-/-}$ muscles were detected by immunohistochemistry. A quantitative analysis of PAX7^{+} cells is shown in the bottom panel. (**B**) WT and *Rage*$^{-/-}$ muscles were analyzed by haematoxylin and eosin stain (H&E) before injury and at the indicated days post-injury. Notice the smaller number and larger size of myofibers in uninjured *Rage*$^{-/-}$ muscle tissue compared with WT tissue (also see E). Also notice the smaller number of regenerating myofibers and the larger number of mononucleated cells at days 5 and 7 post-injury in *Rage*$^{-/-}$ muscle tissue compared with WT tissue. (**C**) Quantitative analysis of centrally nucleated myofibers. (**D**) Same as in (B) except that tissues were subjected to immunohistochemistry for detection of PAX7^{+} cells (figures in panels ± SD, n=3). (**E**) Myofiber cross-sectional area (μm^2) in uninjured WT and *Rage*$^{-/-}$ muscle tissue and at days 7, 14 and 28 post-injury. *Significantly different from internal control (n=3). Scale bars: 100 μm (A,B,D).

by ~50% and were thinner in accordance with the reduced myogenic potential of *Rage*$^{-/-}$ myoblasts; from day 14 to day 28 post-injury, the increase in mean cross-sectional area of *Rage*$^{-/-}$ myofibers was faster, probably because of fusion of a larger number of myoblasts.

By western blotting of muscle tissue homogenates, we showed that uninjured *Rage*$^{-/-}$ tissue contained larger amounts of PAX7 than did WT tissue (Fig. 7A; supplementary material Fig. S3B) in agreement with the immunohistochemical results (Fig. 6D). In WT tissue, PAX7 levels peaked at day 3 post-injury declining thereafter to basal levels; by contrast, PAX7 levels in *Rage*$^{-/-}$ tissue were high from day 1 to day 7 post-injury, and then declined but remained relatively high up to day 28 post-injury (supplementary material Fig. S3B). In addition, MYOD peaked at day 1 post-injury and then declined in WT tissue, whereas it was high from day 3 to day 7 and then disappeared in *Rage*$^{-/-}$ muscle tissue (Fig. 7A; supplementary material Fig. S3B,C). Myogenin levels were high at day 3 post-injury and then declined in WT tissue, whereas nearly constant myogenin levels were detected up to day 7 post-injury in *Rage*$^{-/-}$ tissue, declining thereafter

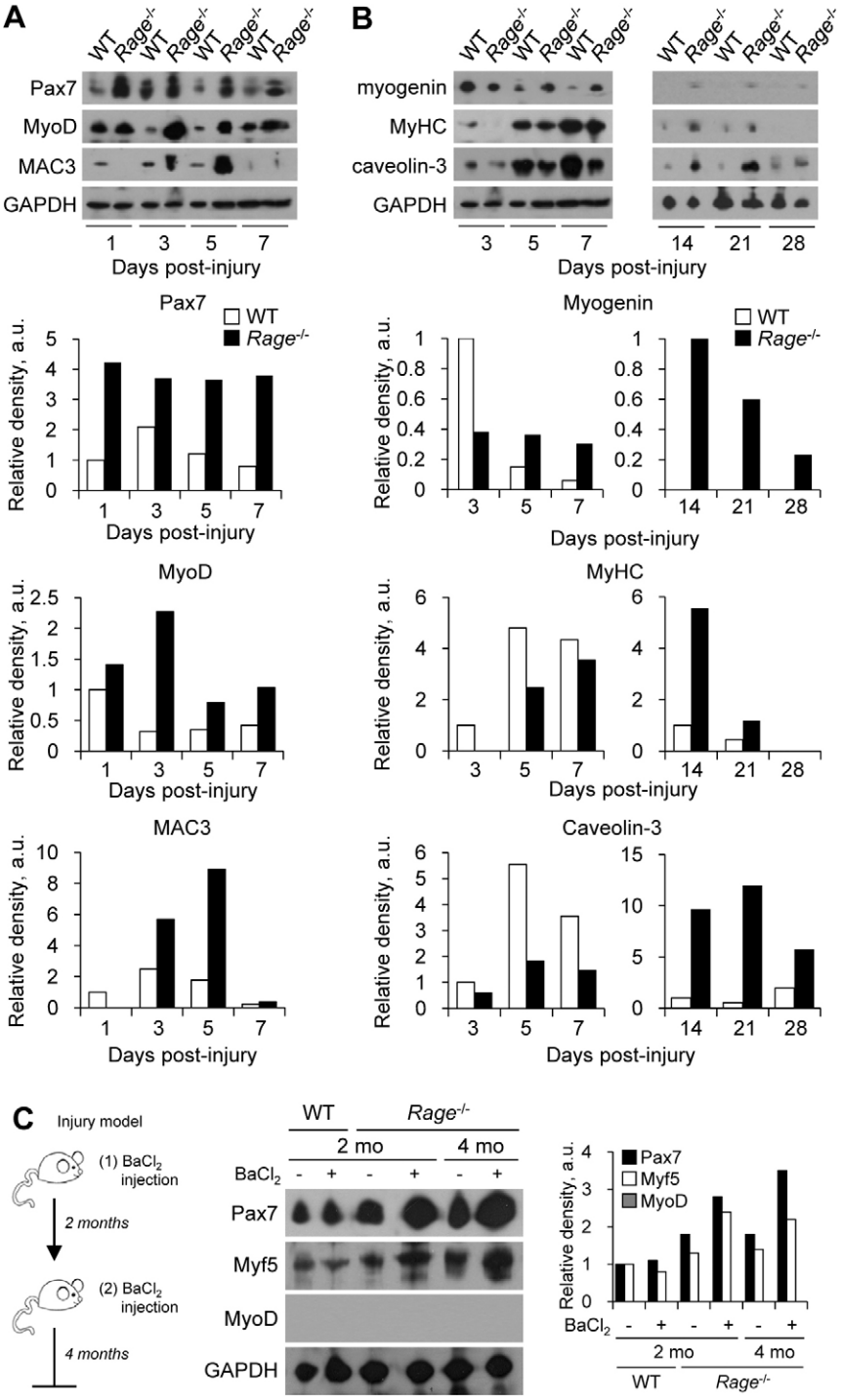

Fig. 7. Time-course of expression of PAX7, MYOD, MAC3, myogenin, MyHC and caveolin-3 in injured WT and *Rage*$^{-/-}$ muscle tissue. (**A**,**B**) After injury, muscle tissue was homogenized at the indicated days post-injury and samples were analyzed by western blotting. *Significantly different from internal control (n=3). (**C**) One month after recovery from injury, *Rage*$^{-/-}$ muscle tissue was subjected to a second round of injury and examined for PAX7, MYF5 and MYOD levels by western blotting of muscle homogenates. Abbreviation: mo, month.

(Fig. 7B; supplementary material Fig. S3B,D). Lastly, whereas developmental MyHC and caveolin-3 appeared in WT tissue at day 1 post-injury, peaked at days 5 and 7 and then disappeared, they were barely detectable in *Rage*$^{-/-}$ tissue during the first 3 days post-injury, then became evident at days 5 and 7, albeit at substantially reduced levels compared with controls, and remained relatively high at days 7 and 14 (MyHC) and days 7 and 28 (caveolin-3) (Fig. 7B; supplementary material Fig. S3B). Thus, the delayed regeneration of *Rage*$^{-/-}$ muscles was probably the result of a prolonged proliferation phase (marked by PAX7) and delayed myoblast differentiation and fusion (marked by MYOD, myogenin, MyHC and caveolin-3) compared with WT tissue. Notably, maximum RAGE levels in injured WT muscle tissue coincided with maximum MyHC and caveolin-3 levels and decreasing PAX7 levels (supplementary material Fig. S3B). The delayed appearance of the activated macrophage marker, MAC3, in injured *Rage*$^{-/-}$ muscles, although at higher levels compared with controls (Fig. 7A; supplementary material Fig. S3B,E), was in line with the notion that RAGE has a crucial role in macrophage migration and activation (Rouhiainen et al., 2004; Yan et al., 2008), and might reflect a more intense and sustained inflammatory response in injured *Rage*$^{-/-}$ muscles than in WT muscles (see Discussion).

Notably, subjecting *Rage*$^{-/-}$ muscles to a second round of injury 2 months after the first injury resulted in even higher levels of PAX7 and MYF5 at 4 months compared with their internal controls (Fig. 7C). This result probably reflected the high proliferation rate and abundance of PAX7, as well as the elevated asymmetric division of *Rage*$^{-/-}$ myoblasts (Fig. 3E); together with results in (Fig. 6), this suggests that RAGE signaling in activated SCs limits myoblast expansion, resulting in the optimization of SC self-renewal and myofiber size and numbers in regenerating muscles.

NF-κB activation induces RAGE expression in injured muscle tissue

We investigated how RAGE was induced in activated SCs upon WT muscle injury. Given that RAGE is induced by NF-κB(p65) in several cell types and the *Rage* promoter contains putative NF-κB recognition sites (Bierhaus et al., 2005), we first analyzed the cellular distribution of phosphorylated NF-κB(p65) in injured muscle tissue. Whereas uninjured WT muscle tissue showed no phosphorylated NF-κB(p65) nuclear localization (Fig. 8Aa), phosphorylated NF-κB(p65) was found in PAX7^{+} (activated satellite) cells at day 1 post-injury, and phosphorylated NF-κB(p65) and PAX7 were colocalized to the nucleus (Fig. 8Ab).

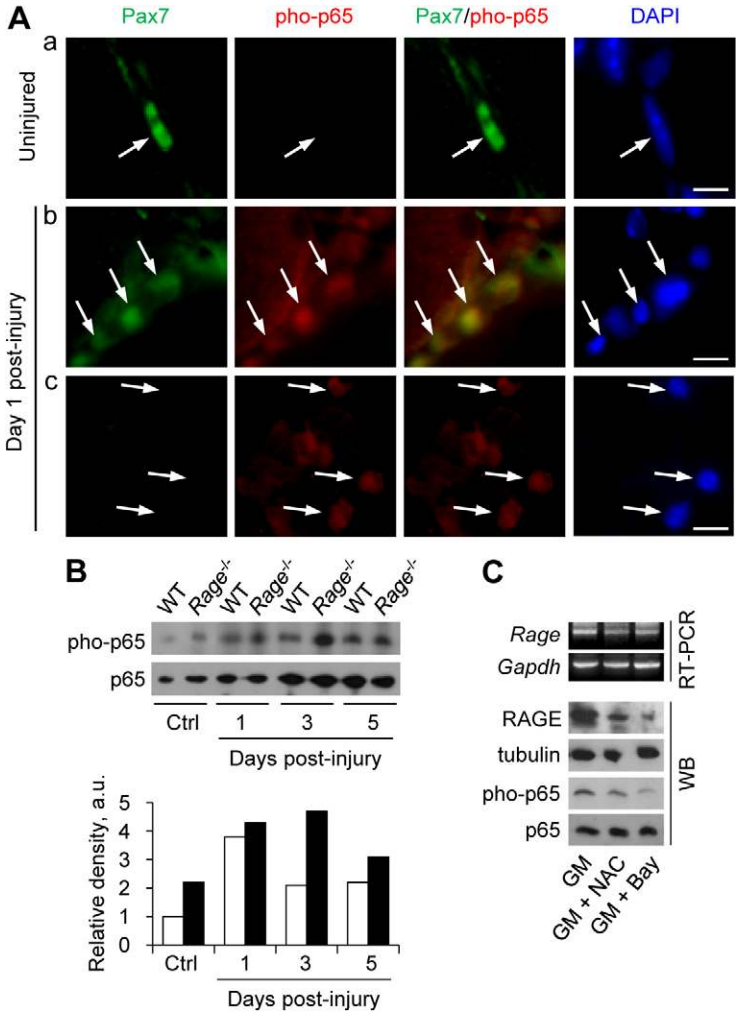

Fig. 8. NF-κB activation induces RAGE expression in injured muscle tissue. (**A**) Immunofluorescence localization of PAX7 and phosphorylated NF-κB (pho-p65) in uninjured and injured WT muscle tissue. No colocalization of PAX7 and phosphorylated NF-κB is seen in the uninjured tissue (a). Arrows point to cells co-expressing PAX7 and NF-κB in the nucleus in the injured tissue at day 1 post-injury (b). Clusters of pho-p65^{+}–PAX7^{-} cells probably representing infiltrating macrophages at day 1 post-injury are also shown (c). Scale bars: 10 μm. (**B**) Western blotting of phosphorylated NF-κB(p65) in homogenates of uninjured and injured WT and *Rage*$^{-/-}$ muscle tissue. (**C**) Primary myoblasts were cultivated in GM for 24 hours in the absence or presence of either the antioxidant, NAC, or the NF-κB inhibitor, Bay 11-7082. Cells were analyzed for *Rage* expression by RT-PCR and for RAGE and phosphorylated NF-κB(p65) levels by western blotting.

Phosphorylated NF-κB(p65) was also found in PAX7^{-} cells (Fig. 8A, c), probably representing infiltrating macrophages. Thus, NF-κB(p65) became activated in SCs upon injury. By western blotting, phosphorylated NF-κB(p65) was relatively high in homogenates of injured WT and *Rage*$^{-/-}$ muscle, with significantly higher levels in *Rage*$^{-/-}$ tissue than in WT tissue beyond day 1 post-injury (Fig. 8B), probably the result of the stronger infiltration of injured *Rage*$^{-/-}$ muscles by activated macrophages and the higher number of activated SCs compared with WT tissue. Treatment of primary WT myoblasts with either the antioxidant, *N*-acetyl cysteine (NAC) or the NF-κB inhibitor, Bay 11-7082, substantially reduced the levels of RAGE and phosphorylated NF-κB(p65) (Fig. 8C), suggesting that damage-induced stress induces RAGE expression in activated SCs via NF-κB(p65).

HMGB1 is released from injured muscles

HMGB1 was restricted to myonuclei in uninjured muscle tissue (supplementary material Fig. S4A); however, it was found in crushed muscle extract (CME) from WT tissue in significantly higher amounts compared with the control (supplementary material Fig. S4B), indicating the release of the protein upon injury. HMGB1 was also restricted to myonuclei in uninjured *Rage*$^{-/-}$ muscles (supplementary material Fig. S4C). However, levels of HMGB1 in muscle homogenates were significantly higher in *Rage*$^{-/-}$ mice than in controls at all time points after injury (supplementary material Fig. S4D): whereas up to day 5 post-injury, this might have depended on the stronger infiltration of *Rage*$^{-/-}$ tissue with macrophages compared with the control (Fig. 7A; supplementary material Fig. S3B,E), beyond this time point the higher abundance of HMGB1 in *Rage*$^{-/-}$ myofibers probably depended on the larger number of myonuclei. Although we cannot exclude the possibility that the large amount of released HMGB1 in injured *Rage*$^{-/-}$ muscles contributed to regeneration by virtue of its ability to attract macrophages (Rouhiainen et al., 2004; Yan et al., 2008; Wang et al., 1999) and mesoangioblasts (Palumbo et al., 2004), the amount was not sufficient to prevent delayed regeneration of injured *Rage*$^{-/-}$ muscles.

Discussion

We have shown that myogenin in differentiating myoblasts represses *Pax7* transcription by associating with regulatory sites in the *Pax7* promoter, that this is permissive for myogenic differentiation to proceed, and that HMGB1–RAGE–p38 MAPK signaling is required for both myogenin induction and myogenin-dependent repression of *Pax7* transcription (Fig. 9A). We have also shown that RAGE is not expressed in adult skeletal muscles, becomes expressed in activated, proliferating SCs and differentiating myoblasts in injured muscles, and is repressed at completion of muscle regeneration. Moreover, myogenin and PAX7 regulate RAGE levels in a positive and negative manner, respectively, in myoblasts (Fig. 9A). Thus, RAGE expression and signaling appear to have an important role in the commitment of myoblasts to differentiation via upregulation of myogenin, which in turn upregulates RAGE expression by a positive feedback mechanism and represses the transcription of *Pax7* (Fig. 9A), a transcription factor that has an important role in SC proliferation and self-renewal and that, if not timely repressed, compromises muscle regeneration. Conversely, PAX7 downregulates RAGE levels (Fig. 9A), so explaining, in part, the lack of RAGE expression in quiescent SCs in uninjured WT muscles and the relatively low RAGE levels in proliferating myoblasts compared with differentiating myoblasts.

Supporting these conclusions, we found that *Rage*$^{-/-}$ myoblasts in DM exhibited reduced p38 MAPK activation and myogenin levels, enhanced PAX7 levels and proliferation, and defective differentiation compared with WT myoblasts. In addition, asymmetric division was elevated in *Rage*$^{-/-}$ myoblasts, in contrast to prevalent symmetric division of primary WT

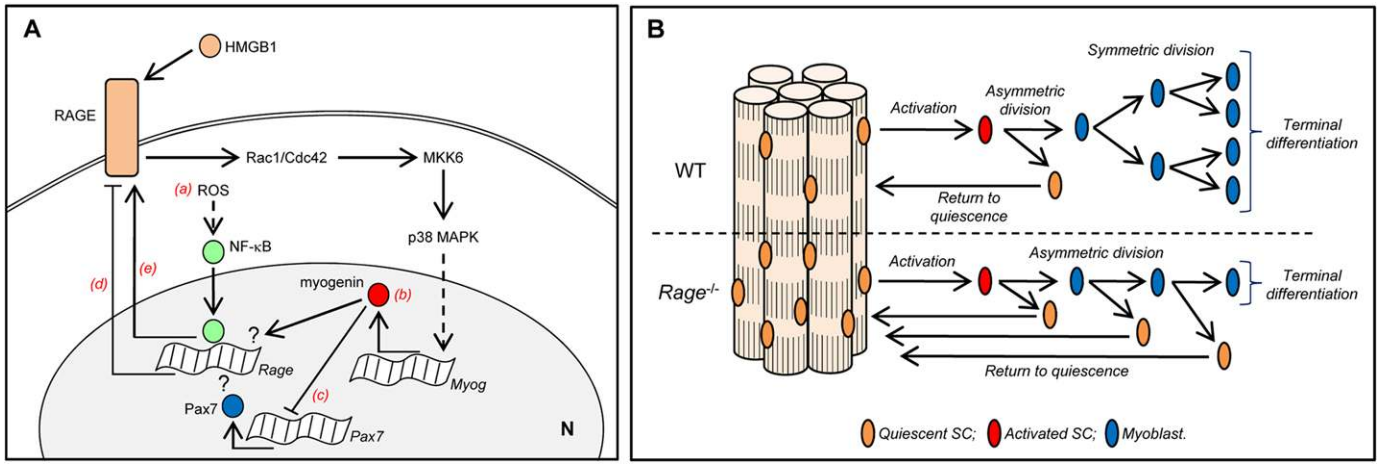

Fig. 9. Schematics of the proposed role of HMGB1–RAGE in muscle regeneration. (**A**) Reactive oxygen species (ROS) produced in activated SCs induce NF-κB-dependent RAGE expression (a). HMGB1-dependent RAGE activation induces p38 MAPK-dependent expression of myogenin (b), which represses PAX7 transcription (c). PAX7 and myogenin regulate RAGE expression in activated SCs in a negative (d) and positive (e) manner, respectively. Whether PAX7- and myogenin-dependent regulation of RAGE is at the transcription level is not known (?). The schema does not take into account the described post-transcriptional (Chen et al., 2010; Dey et al., 2011) and post-translational (Olguin et al., 2007) regulation of PAX7 expression. (**B**) Activated RAGE^{+} SCs divide symmetrically, with a large fraction of myoblasts undergoing differentiation and a minor fraction replenishing the SC reserve pool. Absence of *Rage* causes activated SCs to proliferate faster and promotes asymmetric division, thereby delaying regeneration after muscle injury and increasing the number of myoblasts replenishing the SC reserve pool.

myoblasts. Accordingly, compared with WT muscles, regeneration of *Rage*$^{-/-}$ muscles was delayed and uninjured *Rage*$^{-/-}$ muscles showed higher SC numbers that are even higher at completion of regeneration (Fig. 9B). Thus, excess myoblast proliferation and the elevated myoblast asymmetric division in injured *Rage*$^{-/-}$ muscles delayed regeneration and increased the fraction and number of myoblasts attaining quiescence (Fig. 9B). Moreover, *Rage*$^{-/-}$ myofibers showed a larger mean cross-sectional area and were smaller in number than were WT myofibers. Our results support the conclusion that, following muscle injury, an HMGB1–RAGE–p38 MAPK–myogenin axis physiologically prevents excess myoblast proliferation and maintains the number of self-renewing SCs at a relatively low level via reduction of PAX7 levels in activated SCs, thus accelerating myogenic differentiation and the regeneration process, and optimizing myofiber size and numbers. Our results highlight the fact that, whereas PAX7 was important for SC proliferation and survival, and drove the induction of MYOD in activated and proliferating SCs, with MYOD in turn driving myogenin expression in differentiating myoblasts (Palacios et al., 2010; Sabourin et al., 1999; Seale et al., 2000; Zammit et al., 2006), myogenin reduced PAX7 levels in differentiating myoblasts via a transcriptional mechanism, which adds to previously described post-transcriptional (Chen et al., 2010; Dey et al., 2011) and post-translational (Olguin et al., 2007) mechanisms of PAX7 regulation; in addition, our results show that HMGB1–RAGE has an important role in myogenin-dependent negative regulation of PAX7 levels. It can be anticipated that molecules such as N-cadherin and CDO, which signal to p38 MAPK (Lovett et al., 2006; Takaesu et al., 2006), might downregulate PAX7 in a similar manner to HMGB1–RAGE. Moreover, given that *Rage*$^{-/-}$ muscles were able to regenerate after injury, albeit with at least a 1-week delay, mechanisms should exist that compensate for *Rage* deletion. Given the p38 MAPK-dependent regulation of myogenin and PAX7 expression (de Angelis et al., 2005; Palacios et al., 2010; Perdiguero et al., 2007; Serra et al., 2007), N-cadherin and CDO, from the activation of p38 MAPK (Lovett et al., 2006; Takaesu et al., 2006), and insulin-like growth factors, from the activation of Akt (Chargé and Rudnicki, 2004), could be factors that compensate for the absence of RAGE in injured *Rage*$^{-/-}$ muscles. However, the absence of *Rage* was found to interfere with optimum myofiber numbers and size.

The RAGE ligand and activator, HMGB1, is found in CME, indicating that muscle injury results in its release. HMGB1 is confined to the nucleus in normal physiological conditions, functioning as a regulator of chromatin dynamics (Hock et al., 2007); however, following tissue injury, it moves to the cytoplasm and is then released, acting as a danger signal (Bianchi and Manfredi, 2007; Rauvala and Rouhiainen, 2007). Confirming previous observations (De Mori et al., 2007), we showed that HMGB1 was transiently found within myofibers in injured muscles, pointing to translocation of the protein from the nucleus to the sarcoplasm from where it could be released. Thus, HMGB1 released from the injured muscle tissue and from infiltrating macrophages (Bianchi and Manfredi, 2007; Rauvala and Rouhiainen, 2007) might engage RAGE in activated SCs, thereby stimulating myogenin expression, repressing PAX7 expression and regulating positively the regeneration process (Fig. 9A). HMGB1–RAGE-dependent upregulation of myogenin and downregulation of PAX7 also decreased myoblast proliferation rate and promoted myoblast symmetric division, thereby limiting SC self-renewal (Fig. 9A,B). Indeed, uninjured *Rage*$^{-/-}$ muscles exhibited a higher number of SC than did WT muscles that increased further upon repeated injury–regeneration cycles. Thus, the HMGB1–RAGE–p38 MAPK–myogenin axis regulates SC self-renewal and homeostasis.

RAGE expression in activated and proliferating SCs and in differentiating SCs was dependent on NF-κB(p65) and a p38 MAPK–myogenin axis, respectively. Indeed, rapid NF-κB(p65) activation was detected in mononucleated cells early after injury of WT muscles (Fig. 8) correlating with SC activation (Shi and Garry, 2009); in addition, RAGE was sharply induced in mononucleated cells during the first 24 hours after muscle injury (Fig. 5B). Whereas a fraction of these cells were infiltrating granulocytes and macrophages, another fraction were activated (PAX7^{+}) SCs. RAGE was rapidly expressed in primary WT myoblasts transferred from QM to GM, and antioxidants or inhibition of NF-κB both reduced RAGE expression in proliferating myoblasts. Thus, we propose that damage-induced stress and the consequent NF-κB activation have a major role in the induction of RAGE expression in activated SCs, with further accumulation of RAGE in differentiating myoblasts being dependent on myogenin (Fig. 9A).

Interestingly, during early regeneration phases, the number of infiltrating macrophages in injured muscles was smaller in *Rage*$^{-/-}$ mice than in WT controls, which might contribute to delaying muscle regeneration. It is known that infiltrating macrophages contribute significantly to muscle regeneration by removing cell debris and providing factors that are important for the activation, migration and proliferation of SCs (Robertson et al., 1993; Segawa et al., 2008; Tidball and Villalta, 2010; Tidball and Wehling-Henricks; 2007), and that RAGE is required for efficient macrophage migration (Rouhiainen et al., 2004; Yan et al., 2008). Thus, absence of RAGE might impact muscle regeneration negatively by a double mechanism, that is, by delaying macrophage infiltration of the injured tissue and causing an exaggerated response of SCs, which prolong their proliferation phase at the expense of differentiation and fusion. However, a stronger infiltration of injured muscle tissue with macrophages was observed in *Rage*$^{-/-}$ mice at days 3 and 5 post-injury than in controls, suggesting that the absence of *Rage* results in a more intense, albeit delayed inflammatory response. Thus, RAGE signaling in infiltrating macrophages might mitigate the inflammatory response in degenerating WT muscles, which might contribute significantly to accelerate regeneration. In this respect, absence of *Rage* has been shown to result in an exaggerated inflammatory response in other experimental settings (Sorci et al., 2011; van Zoelen et al., 2009). Whether RAGE signaling has a role in the transition from M_1 to M_2 macrophages at the injury site, an event suggested to have an important role in the progression from the muscle degenerative phase to the regenerative phase (Tidball and Villalta, 2010), remains to be investigated. However, the fact that RAGE levels peak after maximum macrophage infiltration and that RAGE becomes expressed in both PAX7^{+} and myogenin^{+} cells, strongly points to a role for RAGE in proliferating and differentiating SCs during muscle regeneration, independent of its role in macrophages.

How is RAGE repressed in non-fused myoblasts and/or SCs upon completion of regeneration? Our results suggest that PAX7 activity in myogenin^{-} myoblasts destined to become quiescent

causes repression of RAGE expression. Indeed, the *Rage* promoter contains putative recognition sites for *Pax3/7* genes. It is possible that PAX7 represses RAGE expression in a dose-dependent manner in myoblasts, that is, high PAX7 levels, similar to those attained in the absence of myogenin, are required for efficient repression of RAGE expression (Fig. 9A). Moreover, the *Rage* promoter contains putative recognition sites for myogenin: given the p38 MAPK–myogenin dependency of RAGE expression in myoblasts in DM, a decrease in myogenin levels at late regeneration stages (Launay et al., 2001) (supplementary material Fig. S3B) and low or absent NF-κB signaling (Fig. 8) and p38 MAPK activity (Aronson et al., 1998) in normal, resting adult muscle might combine to repress RAGE expression in myoblasts destined to become quiescent SCs and in myofibers (Fig. 9A). However, the mechanism of myogenin- and PAX7-dependent regulation of RAGE expression remains to be determined. We propose that RAGE signaling in injured muscle tissue acts to optimize the number of cells replenishing the SC reserve pool via inhibition of proliferation and stimulation of differentiation. Indeed, $Rage^{-/-}$ myoblasts express high levels of PAX7, have a high proliferation rate and show defective differentiation; in addition, $Rage^{-/-}$ muscles exhibit a larger number of SCs than do WT muscles, probably because of the elevated $Rage^{-/-}$ SC asymmetric division, as outlined above (Fig. 9B). Conversely, expression of RAGE in proliferating myoblasts and/or SCs appears to be required for maintaining PAX7 at a sufficiently low level to avoid excess proliferation. Although future studies should dissect the molecular mechanism governing RAGE expression and repression in SCs depending on the context, our present results suggest that HMGB1–RAGE signaling modulates *Pax7* transcription via p38 MAPK–myogenin, promoting myoblast differentiation, reducing myoblast proliferation and regulating SC self-renewal during muscle regeneration.

Materials and Methods

Reagents

Where specified, cells were treated with either the p38 MAPK inhibitor, SB203580 (5 μM) (Calbiochem), 400 nM HMGB1 antagonist BoxA (HMGBiotech), 40 nM recombinant HMGB1, 10 μg/ml neutralizing polyclonal anti-RAGE antibody (Santa Cruz Biotechnology), 5 mM NAC (Sigma Aldrich) or 2 μM Bay 11-7082 (Calbiochem).

Cell culture

Myoblasts were maintained in high-glucose DMEM supplemented with 20% FBS (Invitrogen), 100 U/ml penicillin and 100 μg/ml streptomycin (GM) in a H_2O-saturated 5% CO_2 atmosphere at 37℃. Primary myoblasts were isolated from 3-day-old WT (C57BL/6) or $Rage^{-/-}$ pups, cultivated as previously described (Neville et al., 1997), and characterized by immunofluorescence using a polyclonal anti-c-Met antibody (Santa Cruz Biotechnology) after fixation with cold methanol for 7 minutes at –20℃. More than 95% of cells were c-Met-positive. Differentiation of C2C12 and primary myoblasts was induced by shifting sub-confluent cultures to antibiotic-containing DMEM supplemented with 2% horse serum (DM). Where required, myoblasts were cultured in methionine-depleted DMEM, 1% FBS (QM) (Kitzmann et al., 1998).

Reverse transcription-PCR and real-time PCR

Total RNA was extracted from C2C12 and primary myoblasts using the TRIzol reagent (Invitrogen) according to the manufacturer's instructions. The following primers were used (denaturation at 95℃ for 30 seconds, annealing at 56℃ for 1 minute and extension at 72℃ for 1 minute): murine RAGE 5′-GGAATTG-TCGATGAGGGGAC-3′ and 5′-CAACAGCTGAATGCCCTCTG-3′; murine PAX7 5′-CGTACCAGTACAGCCAGTATG-3′ and 5′-GTCACTAAGCATGGG-TAGATG-3′; murine myogenin 5′-GCTGTATGAAACATCCCCCTA-3′ and 5′-CGCTGTGGGAGTTGCATT-3′; and murine glyceraldehyde 3-phosphate dehydrogenase (GAPDH) 5′-GCCTTCGCTGTTCCTACCC-3′ and 5′-CAGTG-GGCCCTCAGATGC-3′.

To detect sequences containing putative myogenin recognition sites (5′-TGCCTGG-3′) on the murine *Pax7* promoter (GenBank accession number: AY328081), DNA obtained by ChIP (see below) was analyzed by real-time PCR using the following primer sets: amplified region +90 to +245 (site 1) Forward 5′-GTTGAAAGGTTGCTTGTTCGT-3′ Reverse 5′-AGTGCCTGCTTGACTTTGCT-3′; amplified region +758 to +922 (site 2) Forward 5′-CCACTTTATGTTGG-GTGGAGA-3′ Reverse 5′-CATCCCCTTCTCCTCCTCTT-3′; amplified region +1925 to +2119 (site 3) (R) Forward 5′-CCTGGACTCCCACTTTCTCTG-3′ Reverse 5′-CAGGGCTTTTCATTAGGTAGCA-3′; amplified region +2303 to +2459 (site 4) Forward 5′-AGCGTGGGTTACCACATAGC-3′ Reverse 5′-CATGCTGTGCTCATCTCTGAA-3′; amplified region +4231 to +4408 (site 5) (R) Forward 5′-ACTCCGAATCTTTCTGCTTGG-3′ Reverse 5′-TGCCTATA-GCTGGCACTCAAT-3′; and amplified region +8024 to +8213 (site 6) (R) Forward 5′-CAAGGTTACCAGCTGGGTGT-3′ Reverse 5′-TCAATGGGGAGG-GTGTAATG-3′, where (R) indicates that the myogenin recognition site was on the reverse orientation (5′-CCAGGCA-3′). DNA was mixed with Real Master Mix and SYBR solution (Eppendorf) in a reaction volume of 20 μl. Reaction mixtures were incubated in a thermocycler (Stratagene) and analyzed by the Multiplex Quantitative PCR System.

Western blotting

Muscle tissue was homogenized in 50 mM Tris pH 7.4, 150 mM NaCl, 1% Triton X-100, in the presence of a mixture of protease inhibitors (Roche Applied Science). The amount of protein in each sample was determined by Bradford assay. Equal amounts of protein were size separated by SDS-PAGE. C2C12 and primary myoblasts were lysed and the cell lysates subjected to western blotting, as previously described (Sorci et al., 2003). CME was obtained as previously described (Chen and Quinn, 1992). HMGB1 in CME was analyzed by western blotting after TCA precipitation. The following antibodies were used: polyclonal anti-RAGE (1:1000, Santa Cruz Biotechnology), monoclonal anti-PAX7 (1:500, R&D Systems), monoclonal anti-MYOD (1:500, Santa Cruz Biotechnology), monoclonal anti-myogenin (1:1000, BD Biosciences), polyclonal anti-MYF5 (1:1000, Santa Cruz Biotechnology), monoclonal anti-MyHC (1:1000, Novocastra), monoclonal anti-caveolin-3 (1:2000, BD Biosciences), polyclonal anti-MAC3 (1:1000, BD Biosciences), polyclonal anti-phosphorylated (Ser536) NF-κB(p65) (1:1000, Cell Signaling), polyclonal anti-NF-κB(p65) (1:1000, Santa Cruz Biotechnology), anti-HMGB1 (1:1000, R&D Systems), polyclonal anti-GAPDH (1:5000, Santa Cruz Biotechnology) monoclonal anti-α-tubulin (1:10,000, Sigma Aldrich), polyclonal anti-phosphorylated (Thr180/Tyr182) p38 MAPK (1:1000, Cell Signaling Technology), polyclonal anti-p38 MAPK (1:2000, Cell Signaling Technology), polyclonal anti-phosphorylated (Thr202/Tyr204) ERK1/2 (1:2000, Cell Signaling Technology), and polyclonal anti-ERK1/2 (1:20,000, Sigma Aldrich). The immune reaction was developed by enhanced chemiluminescence (SuperSignal West Femto Maximum or SuperSignal West Pico, both from Pierce).

ChIP

C2C12 or primary myoblasts at a density of 1.0×10^6 were cultured for 48 hours in either GM or DM, and processed using a ChIP Assay Kit (Upstate, Cell Signaling Solution) as recommended by the manufacturer. Lysates were separated into two aliquots and immunoprecipitated with 3 μg of polyclonal anti-myogenin antibody (Santa Cruz Biotechnology) or pre-immune rabbit serum IgG (Sigma Aldrich). Immunoprecipitated DNA fragments were recovered using phenol and/or chloroform and ethanol precipitation. Three μl of each eluate or total DNA (input) were used in real-time PCR reactions. See above for primer sets of the promoter of murine *Pax7* gene containing a putative myogenin recognition site.

Transfection and gene knockdown

Transient transfections were carried out using jetPEI™ (Polyplus Transfection), as recommended by the manufacturer. Briefly, C2C12 or WT and $Rage^{-/-}$ primary myoblasts were transfected with pEMSV-myogenin, pcDNA3–RAGE, pcDNA3–RAGEΔcyto, PAX7d–pcDNA3 or an empty vector. For luciferase reporter assay, cells were transfected with a luciferase reporter vector under the control of the –4800 bp region of the human *PAX7* promoter (pGL3b –4800) (Murmann et al., 2000). Transfection efficiency was ~30%. After 24 hours, the cells were harvested to measure luciferase activity using the Luciferase Assay System (Promega).

Subconfluent C2C12 myoblasts were transfected with Control siRNA-A (Santa Cruz Biotechnology), PAX7 siRNA(m) (Santa Cruz Biotechnology) or On-target plus SMART pool mouse myogenin (Thermo Scientific Dharmacon) using Interferin™ (Polyplus Transfection) according to the manufacturer's instructions. Transfection efficiency was ~70%. After cultivation, the cells were subjected to either reverse transcription (RT)-PCR or western blotting, as described in the legends to pertinent figures.

Cell proliferation

Cell proliferation was measured by either viable cell count, BrdU incorporation assay (Riuzzi et al., 2011) or calculation of population doubling level [$pdl = \log_{10}(N/n)/\log_2$].

Primary myoblast division assay

WT C57BL/6 and *Rage*$^{-/-}$ primary myoblasts were labeled with Vybrant® DiI Cell-Labeling Solution (Invitrogen) according to the manufacturer's instructions. To ensure that the cells took up the dye, a fraction of labeled cells were washed in PBS after a 15-minute recovery time and analyzed using a FACScan flow cytometer (Becton Dickinson), equipped with a 488-nm laser (Enterprise Coherent) and a 575/26 BP optical filter (FL2 channel). Under these conditions, we usually observed 100% labeling of cells. Labeled cells were cultured in GM for another 2 or 6 days and then analyzed in the same manner. Dead cells were gated out by size (forward scatter). Percentages of positive cells were calculated after subtracting the background in the isotypic control sample. Labeled cells were also viewed using a Leica DMRB epifluorescence microscope.

Co-immunoprecipitation

C2C12 myoblasts cultivated for 6, 24 or 48 hours in DM were lysed in buffer containing 50 mM Tris-HCl (pH 7.4), 150 mM NaCl, 1% Triton X-100, 1 mM $CaCl_2$, 10 mM NaF and 1 mM sodium orthovanadate in the presence of a mixture of protease inhibitors (Roche Applied Science). Solubilized proteins were subjected to immunoprecipitation using either a polyclonal anti-myogenin antibody (Santa Cruz Biotechnology, 2 µg/mg total protein) or non-immune rabbit IgG. The immunoprecipitates were subjected to western blotting for detection of PAX7 and myogenin.

Animal husbandry

Approval of use of animals was obtained from the Ethics Committee of the Perugia University and the Ministero della Salute, Italy.

Animals, experimental muscle injury and histological analyses

C57BL/6 mice were obtained from Charles River. *Rage*$^{-/-}$ mice were obtained from Angelika Bierhaus (Heidelberg, Germany). Injury of muscles was performed by $BaCl_2$ injection (Caldwell et al., 1990) in the tibialis anterior muscle of 8-week-old *Rage*$^{-/-}$ and WT mice, under zolazepam–tiletamine anesthesia. Briefly, 50 µl of an aqueous 1.2% (w/v) $BaCl_2$ solution was injected along the whole length of the left tibialis anterior muscles. Controlateral muscles were injected with vehicle and used as controls. Before injury and at various time points after $BaCl_2$ injection, control and treated tibialis anterior muscles were removed, fixed in 4% formalin in PBS (pH 7.2) and paraffin embedded. Muscle cross-sections measuring 4 µm were obtained and stained with haematoxylin and/or eosin. To quantify the extent of muscle regeneration, sections at 100 µm intervals for each muscle were analyzed and the total number of centrally nucleated myofibers per section was manually counted by three independent operators. Myofiber cross-sectional area was measured using the Cell P Analysis Imaging Processing Olympus software. Values reported are given as mean ± SD obtained from multiple animals. In some experiments, muscle injury with $BaCl_2$ was performed twice (Fig. 7C).

Immunohistochemistry, immunofluorescence and immunocytochemistry

Paraffin sections of control or treated tibialis anterior muscles were cut at 4 µm, deparaffinized with xylene and rehydrated in a graded ethanol series. Antigen retrieval was obtained by boiling for 2 hours in 10 mM citric acid buffer (pH 6.0), and depletion of endogenous peroxidase was accomplished by treatment with 3% H_2O_2. Sections were washed with TBS, pH 7.4, incubated for 1 hour with Blocking Buffer [BB, TBS containing 0.01% Tween-20 (T-TBS) and 10% HS] and then probed with the following antibodies: goat polyclonal anti-RAGE (Santa Cruz Biotechnology), mouse monoclonal anti-PAX7 (R&D Systems), mouse monoclonal anti-MYOD (clone 5.8A, Santa Cruz Biotechnology), mouse monoclonal anti-myogenin (Santa Cruz Biotechnology), mouse monoclonal anti-HMGB1 (R&D Systems), or rat polyclonal anti-MAC3 (BD Biosciences). The antibodies were diluted (1:50) in BB and the sections incubated overnight in a humid chamber at 4℃. After several washings with T-TBS, the sections were incubated with appropriate second biotinylated antibodies (1:500 dilution; Vector Laboratories) for 1 hour in BB. The sections were then rinsed with T-TBS, incubated for 45 minutes with Vectastain ABC reagents (Vector Laboratories), washed again with T-TBS and incubated with 0.01% 3,3-diaminobenzidine tetrahydrochloride, 0.006% H_2O_2 in 50 mM Tris-HCl (pH 7.4). Nuclei were counterstained with haematoxylin. The sections were then dehydrated and mounted with EuKitt mounting medium (Electron Microscopy Sciences). Slices were analyzed and photographed with a bright field microscope (Olympus BX51) equipped with a digital camera.

Double-immunofluorescence reactions on tissue slices were performed as above except that PBS, pH 7.4, instead of T-TBS and a different BB (i.e. 0.4% Triton-X-100, 10% donkey serum and 1% BSA in PBS) were used. The primary antibodies used (1:20 in BB) were goat polyclonal anti-RAGE (Santa Cruz Biotechnology), mouse monoclonal anti-PAX7 (R&D Systems), mouse monoclonal anti-myogenin (Santa Cruz Biotechnology) and/or polyclonal anti-phosphorylated NF-κB(p65). The secondary antibodies were donkey anti-mouse-Alexa-Fluor-488-conjugated (Invitrogen), donkey anti-goat-Alexa-Fluor-594-conjugated (Invitrogen) and goat anti-rabbit rhodamine-conjugated (Sigma Aldrich).

For double-immunofluorescence staining of C2C12 myoblasts, cells were grown on glass coverslips, fixed in 4% paraformaldehyde in PBS and processed with BB, primary and secondary antibodies as above. Nuclei were counterstained with DAPI. After rinsing, samples were mounted in fluorescent mounting medium (Dako Corporation) and viewed in an epifluorescence microscope (Leica DMRB) equipped with a digital camera.

MyHC was detected by immunocytochemistry as previously described (Sorci et al., 2003).

Statistical analysis

Each experiment was repeated at least three times. Representative experiments are shown unless stated otherwise. The data were subjected to analysis of variance (ANOVA) with SNK post-hoc analysis using a statistical software package (GraphPad Prism version 4.00, GraphPad).

Acknowledgements

We wish to thank Angelika Bierhaus (Heidelberg, Germany) for providing *Rage*$^{-/-}$ mice, Heikki Rauvala (Helsinki, Finland) for providing HMGB1, RAGE and RAGEΔcyto expression vectors, Eyal Bengal (Haifa, Israel) for providing the myogenin-luc gene reporter, Bradley Olwin (Boulder, CO) for providing the PAX7 expression vector, and Beat Schäfer (Zurich, Switzerland) for providing the pGL3b-4800 *PAX*7-luc construct.

Funding

The authors were supported by the Association Française contre les Myopathies (Project 12992); Associazione Italiana per la Ricerca sul Cancro (Project 6021); Ministero dell'Università e della Ricerca [grant numbers PRIN 2004054293, 2007LNKSYS and 2007AWZTHH_004]; and Fondazione Cassa di Risparmio di Perugia [grant numbers 2004.0282.020, 2007.0218.020 and 2009.020.0021]. R. S. is recipient of a fellowship from Consorzio Interuniversitario per le Biotecnologie. The authors declare no conflict of interest.

Supplementary material available online at
http://jcs.biologists.org/lookup/suppl/doi:10.1242/jcs.092163/-/DC1

References

Andersson, U., Erlandsson-Harris, H., Yang, H. and Tracey, K. J. (2002). HMGB1 as a DNA-binding cytokine. *J. Leukoc. Biol.* **72**, 1084-1091.

Aronson, D., Wojtaszewski, J. F., Thorell, A., Nygren, J., Zangen, D., Richter, E. A., Ljungqvist, O., Fielding, R. A. and Goodyear, L. J. (1998). Extracellular-regulated protein kinase cascades are activated in response to injury in human skeletal muscle. *Am. J. Physiol.* **275**, C555-C561.

Bianchi, M. E. and Manfredi, A. A. (2007). High-mobility group box 1 (HMGB1) protein at the crossroads between innate and adaptive immunity. *Immunol. Rev.* **220**, 35-46.

Bierhaus, A., Humpert, P. M., Morcos, M., Wendt, T., Chavakis, T., Arnold, B., Stern, D. M. and Nawroth, P. P. (2005). Understanding RAGE, the receptor for advanced glycation end products. *J. Mol. Med.* **83**, 876-886.

Brack, A. S., Conboy, M. J., Roy, S., Lee, M., Kuo, C. J., Keller, C. and Rando, T. A. (2007). Increased Wnt signaling during aging alters muscle stem cell fate and increases fibrosis. *Science* **317**, 807-810.

Buckingham M. (2006). Myogenic progenitor cells and skeletal myogenesis in vertebrates. *Curr. Opin. Genet. Dev.* **16**, 525-532.

Caldwell, C. J., Mattey, D. L. and Weller, R. O. (1990). Role of the basement membrane in the regeneration of skeletal muscle. *Neuropathol. Appl. Neurobiol.* **16**, 225-238.

Chargé, S. B. and Rudnicki, M. A. (2004). Cellular and molecular regulation of muscle regeneration. *Physiol. Rev.* **84**, 209-238.

Chen, G. and Quinn, L. S. (1992). Partial characterization of skeletal myoblast mitogens in mouse crushed muscle extract. *J. Cell. Physiol.* **153**, 563-574.

Chen, J. F., Tao, Y., Li, J., Deng, Z., Yan, Z., Xiao, X. and Wang, D. Z. (2010). microRNA-1 and microRNA-206 regulate skeletal muscle satellite cell proliferation and differentiation by repressing Pax7. *J. Cell Biol.* **190**, 867-879.

Collins, C. A., Gnocchi, V. F., White, R. B., Boldrin, L., Perez-Ruiz, A., Relaix, F., Morgan, J. E. and Zammit, P. S. (2009). Integrated functions of Pax3 and Pax7 in the regulation of proliferation, cell size and myogenic differentiation. *PLoS ONE* **4**, e4475.

de Angelis, L., Zhao, J., Andreucci, J. J., Olson, E. N., Cossu, G. and McDermott, J. C. (2005). Regulation of vertebrate myotome development by the p38 MAP kinase-MEF2 signaling pathway. *Dev. Biol.* **283**, 171-179.

De Mori, R., Straino, S., Di Carlo, A., Mangoni, A., Pompilio, G., Palumbo, R., Bianchi, M. E., Capogrossi, M. C. and Germani, A. (2007). Multiple effects of high mobility group box protein 1 in skeletal muscle regeneration. *Arterioscler. Thromb. Vasc. Biol.* **27**, 2377-2383.

Dey, B. K., Gagan, J. and Dutta, A. (2011). miR-206 and -486 induce myoblast differentiation by downregulating Pax7. *Mol. Cell. Biol.* **31**, 203-214.
Hock, R., Furusawa, T., Ueda, T. and Bustin, M. (2007). HMG chromosomal proteins in development and disease. *Trends Cell. Biol.* **17**, 72-79.
Kitzmann, M., Carnac, G., Vandromme, M., Primig, M., Lamb, N. J. and Fernandez, A. (1998). The muscle regulatory factors MyoD and myf-5 undergo distinct cell cycle-specific expression in muscle cells. *J. Cell Biol.* **142**, 1447-1459.
Krishnamurthy, K., Wang, G., Rokhfeld, D. and Bieberich, E. (2008). Deoxycholate promotes survival of breast cancer cells by reducing the level of pro-apoptotic ceramide. *Breast Cancer Res.* **10**, R106.
Kuang, S., Chargé, S. B., Seale, P., Huh, M. and Rudnicki, M. A. (2006). Distinct roles for Pax7 and Pax3 in adult regenerative myogenesis. *J. Cell Biol.* **172**, 103-113.
Kuang, S., Gillespie, M. A. and Rudnicki, M. A. (2008). Niche regulation of muscle satellite cell self-renewal and differentiation. *Cell Stem Cell* **2**, 22-31.
Launay, T., Armand, A. S., Charbonnier, F., Mira, J. C., Donsez, E., Gallien, C. L. and Chanoine, C. (2001). Expression and neural control of myogenic regulatory factor genes during regeneration of mouse soleus. *J. Histochem. Cytochem.* **49**, 887-899.
Lovett, F. A., Gonzalez, I., Salih, D. A., Cobb, L. J., Tripathi, G., Cosgrove, R. A., Murrell, A., Kilshaw, P. J. and Pell, J. M. (2006). Convergence of Igf2 expression and adhesion signalling via RhoA and p38 MAPK enhances myogenic differentiation. *J. Cell Sci.* **119**, 4828-4840.
Murmann, O. V., Niggli, F. and Schäfer, B. W. (2000). Cloning and characterization of the human PAX7 promoter. *Biol. Chem.* **381**, 331-335.
Neville, C., Rosenthal, N., McGrew, M., Tsakiris, T., Parthimos, N. and Hauschka, S. (1997). Skeletal muscle cultures. *Methods Cell Biol.* **52**, 85-116.
Olguin, H. C. and Olwin, B. B. (2004). Pax-7 up-regulation inhibits myogenesis and cell cycle progression in satellite cells: a potential mechanism for self-renewal. *Dev. Biol.* **275**, 375-388.
Olguin, H. C., Yang, Z., Tapscott, S. J. and Olwin, B. B. (2007). Reciprocal inhibition between Pax7 and muscle regulatory factors modulates myogenic cell fate determination. *J. Cell Biol.* **177**, 769-779.
Palacios, D., Mozzetta, C., Consalvi, S., Caretti, G., Saccone, V., Proserpio, V., Marquez, V. E., Valente, S., Mai, A., Forcales, S. V. et al. (2010). TNF/p38α/polycomb signaling to Pax7 locus in satellite cells links inflammation to the epigenetic control of muscle regeneration. *Cell Stem Cell* **7**, 455-469.
Palumbo, R., Sampaolesi, M., De Marchis, F., Tonlorenzi, R., Colombetti, S., Mondino, A., Cossu, G. and Bianchi, M. E. (2004). Extracellular HMGB1, a signal of tissue damage, induces mesoangioblast migration and proliferation. *J. Cell Biol.* **164**, 441-449.
Perdiguero, E., Ruiz-Bonilla, V., Gresh, L., Hui, L., Ballestar, E., Sousa-Victor, P., Baeza-Raja, B., Jardí, M., Bosch-Comas, A., Esteller, M. et al. (2007). Genetic analysis of p38 MAP kinases in myogenesis: fundamental role of p38alpha in abrogating myoblast proliferation. *EMBO J.* **26**, 1245-1256.
Rauvala, H. and Rouhiainen, A. (2007). RAGE as a receptor of HMGB1 (Amphoterin): roles in health and disease. *Curr. Mol. Med.* **7**, 725-734.
Relaix, F., Rocancourt, D., Mansouri, A. and Buckingham, M. (2005). A Pax3/Pax7-dependent population of skeletal muscle progenitor cells. *Nature* **435**, 948-953.
Relaix, F., Montarras, D., Zaffran, S., Gayraud-Morel, B., Rocancourt, D., Tajbakhsh, S., Mansouri, A., Cumano, A. and Buckingham, M. (2006). Pax3 and Pax7 have distinct and overlapping functions in adult muscle progenitor cells. *J. Cell Biol.* **172**, 91-102.
Riuzzi, F., Sorci, G. and Donato, R. (2006). The amphoterin/RAGE pair modulates myoblast proliferation, apoptosis, adhesiveness, migration and invasiveness. Functional inactivation of RAGE in L6 myoblasts results in tumor formation in vivo. *J. Biol. Chem.* **281**, 8242-8253.
Riuzzi, F., Sorci, G. and Donato, R. (2007). RAGE expression in rhabdomyosarcoma cells results in myogenic differentiation and reduced proliferation, migration, invasiveness, and tumor growth. *Am. J. Pathol.* **171**, 947-961.
Riuzzi, F., Sorci, G. and Donato, R. (2011). S100B protein regulates myoblast proliferation and differentiation by activating FGFR1 in a bFGF-dependent manner. *J. Cell Sci.* **124**, 2389-2400.
Robertson, T. A., Maley, M. A., Grounds, M. D. and Papadimitriou, J. M. (1993). The role of macrophages in skeletal muscle regeneration with particular reference to chemotaxis. *Exp. Cell Res.* **207**, 321-331.
Rouhiainen, A., Kuja-Panula, J., Wilkman, E., Pakkanen, J., Stenfors, J., Tuominen, R. K., Lepäntalo, M., Carpén, O., Parkkinen, J. and Rauvala, H. (2004). Regulation of monocyte migration by amphoterin (HMGB1). *Blood* **104**, 1174-1182.
Sabourin, L. A., Girgis-Gabardo, A., Seale, P., Asakura, A. and Rudnicki, M. A. (1999). Reduced differentiation potential of primary MyoD$^{-/-}$ myogenic cells derived from adult skeletal muscle. *J. Cell Biol.* **144**, 631-643.
Schmidt, A. M., Yan, S. D., Yan, S. F. and Stern, D. M. (2001). The multiligand receptor RAGE as a progression factor amplifying immune and inflammatory responses. *J. Clin. Invest.* **108**, 949-955.
Seale, P., Sabourin, L. A., Girgis-Gabardo, A., Mansouri, A., Gruss, P. and Rudnicki, M. A. (2000). Pax7 is required for the specification of myogenic satellite cells. *Cell* **102**, 777-786.
Segawa, M., Fukada, S., Yamamoto, Y., Yahagi, H., Kanematsu, M., Sato, M., Ito, T., Uezumi, A., Hayashi, S., Miyagoe-Suzuki, Y. et al. (2008). Suppression of macrophage functions impairs skeletal muscle regeneration with severe fibrosis. *Exp. Cell Res.* **314**, 3232-3244.
Serra, C., Palacios, D., Mozzetta, C., Forcales, S. V., Morante, I., Ripani, M., Jones, D. R., Du, K., Jhala, U. S., Simone, C. et al. (2007). Functional interdependence at the chromatin level between the MKK6/p38 IGF1/PI3K/AKT pathways during muscle differentiation. *Mol. Cell* **28**, 200-213.
Shi, X. and Garry, D. J. (2009). Muscle stem cells in development, regeneration, and disease. *Genes Dev.* **20**, 1692-1708.
Sorci, G., Agneletti, A. L., Riuzzi, F., Marchetti, C. and Donato, R. (2003). S100B inhibits myogenic differentiation and myotube formation in a RAGE-independent manner. *Mol. Cell. Biol.* **23**, 4870-4881.
Sorci, G., Riuzzi, F., Arcuri, C., Giambanco, I. and Donato, R. (2004). Amphoterin stimulates myogenesis and counteracts the antimyogenic factors basic fibroblast growth factor and S100B via RAGE binding. *Mol. Cell. Biol.* **24**, 4880-4894.
Sorci, G., Giovannini, G., Riuzzi, F., Bonifazi, P., Zelante, T., Zagarella, S., Bistoni, F., Donato, R. and Romani, L. (2011). The danger signal S100B integrates pathogen- and danger-sensing pathways to restrain inflammation. *PLoS Pathog.* **7**, e1001315.
Takaesu, G., Kang, J. S., Bae, G. U., Yi, M. J., Lee, C. M., Reddy, E. P. and Krauss, R. S. (2006). Activation of p38α/β MAPK in myogenesis via binding of the scaffold protein JLP to the cell surface protein Cdo. *J. Cell Biol.* **175**, 383-388.
Tedesco, F. S., Dellavalle, A., Diaz-Manera, J., Messina, G. and Cossu, G. (2010). Repairing skeletal muscle: regenerative potential of skeletal muscle stem cells. *J. Clin. Invest.* **120**, 11-19.
Tidball, J. G. and Wehling-Henricks, M. (2007). Macrophages promote muscle membrane repair and muscle fibre growth and regeneration during modified muscle loading in mice in vivo. *J. Physiol.* **578**, 327-336.
Tidball, J. G. and Villalta, S. A. (2010). Regulatory interactions between muscle and the immune system during muscle regeneration. *Am. J. Physiol. Regul. Integr. Comp. Physiol.* **298**, R1173-R1187.
van Zoelen, M. A., Schmidt, A. M., Florquin, S., Meijers, J. C., de Beer, R., de Vos, A. F., Nawroth, P. P., Bierhaus, A. and van der Poll, T. (2009). Receptor for advanced glycation end products facilitates host defense during Escherichia coli-induced abdominal sepsis in mice. *J. Infect. Dis.* **200**, 765-773.
Wang, H., Bloom, O., Zhang, M., Vishnubhakat, J. M., Ombrellino, M., Che, J., Frazier, A., Yang, H., Ivanova, S., Borovikova, L. et al. (1999). HMG-1 as a late mediator of endotoxin lethality in mice. *Science* **285**, 248-251.
Yan, S. F., Ramasamy, R. and Schmidt, A. M. (2008). Mechanisms of disease: advanced glycation end-products and their receptor in inflammation and diabetes complications. *Nat. Clin. Pract. Endocrinol. Metab.* **4**, 285-293.
Yoshida, N., Yoshida, S., Koishi, K., Masuda, K. and Nabeshima, Y. (1998). Cell heterogeneity upon myogenic differentiation: down-regulation of MyoD and Myf-5 generates "reserve cells". *J. Cell Sci.* **111**, 769-779.
Zammit, P. S., Golding, J. P., Nagata, Y., Hudon, V., Partridge, T. A. and Beauchamp, J. R. (2004). Muscle satellite cells adopt divergent fates: a mechanism for self-renewal? *J. Cell Biol.* **166**, 347-357.
Zammit, P. S., Relaix, F., Nagata, Y., Ruiz, A. P., Collins, C. A., Partridge, T. A. and Beauchamp, J. R. (2006). Pax7 and myogenic progression in skeletal muscle satellite cells. *J. Cell Sci.* **119**, 1824-1832.